

OPTIMAL PRODUCTION PLANNING AND HEDGING FOR BIO-ENERGY INDUSTRY

A Dissertation

Presented to the Faculty of the Graduate School

of Cornell University

in Partial Fulfillment of the Requirements for the Degree of

Doctor of Philosophy

by

Lingfeng Cheng

August 2017

© 2017 Lingfeng Cheng
ALL RIGHTS RESERVED

OPTIMAL PRODUCTION PLANNING AND HEDGING FOR BIO-ENERGY INDUSTRY

Lingfeng Cheng, Ph.D.

Cornell University 2017

Renewable energy has become a viable alternative to fossil fuel due to its environmental benefits, sustainability, and potential social welfare. Bioethanol, as one of the dominant renewable energy sources, have become a short and medium term solution to reduce our dependency on fossil fuel. A biorefinery is a process that embraces a wide range of technology to convert biomass to value added products such as ethanol, hydrogen, and industrial chemicals. Based on the source of feedstock, biorefineries has evolved through three main phases. The first generation of bioethanol is produced from corn and has been the main source of ethanol in US. Several second generation bioethanol plants have been established at pilot scale using feedstocks such as switchgrasses, woody crops and agriculture residues. A third generation of biorefinery producing bioproducts from algae is believed to have potential, but continues to face challenges in commercial feasibility.

There is a growing consensus that carbon emission, if left unchecked, will lead to major changes in the climate system. As a result, governments are under growing pressure to enact legislation to curb the amount of carbon emissions, and energy producers worldwide are obliged to adjust their production policy in response to the change of carbon emission policy.

A challenge associated with both corn and ethanol, is the existing drastic price fluctuations on the commodity markets. For a biorefinery that consumes

corn and produces ethanol, if fully exposed to this price variation, could suffer from great financial loss resulting from the sudden price changes. Therefore, managing financial risk becomes an essential task for a biorefinery. Financial derivatives, such as forwards, futures, swap and options are commonly used tools in financial risk management, which help to transfer the price uncertainty to the counterparty based on mutual financial agreement.

Motivated by the complications of environmental policy and financial uncertainty, the goal of this work is the development of a systematic optimization framework to help manage the financial risk for both first generation and second generation biorefineries. The solution will maximize economic viability of the process under a specified risk level and with specified carbon tax constraints. Considering different time horizons and derivative types, the framework consists of a price model, a process model, and a hedging model, which interact to generate the optimal operational and hedging strategies. The approach will be demonstrated with results from case studies and is also validated from back-testing with historical price data.

BIOGRAPHICAL SKETCH

Lingfeng Cheng is a 5th year Ph.D. Candidate in the department of Chemical and Biomolecular Engineering. He completed his Bachelor of Science in Material Science and Engineering at University of Science and Technology of China. Since his junior, he has had a strong interest in quantitative modeling and optimization, which motivated him to pursue his graduate study in Cornell University with Professor C. Lindsay Anderson. At Cornell, his research has focused on formulating the optimal production and hedging decisions for a biorefinery.

To my parents Wenjun Ba and Feiyue Cheng.

ACKNOWLEDGEMENTS

First, I would like to thank my advisor Professor C. Lindsay Anderson. It has been and will always be an honor to be her student. Lindsay is someone you will instantly love and never forget once you meet her. I still deeply remember the October five years ago, when I was fresh into the graduate school, anxiously looking for an advisor who can guide me in the area of applied modeling and optimization, Lindsay presented me the great potential of integrating optimal decision making in the renewable energy area. This choice has shaped both my research interest and career path. She is lively, enthusiastic, energetic, and smart. Whenever I encountered obstacles in my research problems, a discussion with Lindsay is always fruitful and relieving. She also has taught me what really means to be a good applied researcher. A clear problem definition and an applicable strategy worth far more than a complicate model.

Second, I am thankful to my committee member, Professor Jefferson William Tester, and Professor. Beth Ahner. Jeff's deep knowledge in the renewable energy industry is always a valuable asset for me to pinpoint the key problems in this industry. The facts as well as the skills I have gained from his renewable energy classes will serve as a lifelong benefit for me. The benign and warm-hearted Beth has always been supportive and has given me the freedom to explore various projects without objection. Although serving as the senior associate dean, she still spares her valuable time on her responsibility in my committee. I deeply appreciate her commitment.

Moreover, I would like to thank my lab members, Maureen, Gabriela, Luckny, Amandeep and Jialin. Maureen serves as a great mentor in my career. Without her, I would never be able to have the chance to interview with the Insight Data Science Fellowship Program. Gabriela was always helpful, read-

ily available anytime when I had technical difficulties in my model. She also brought python to our lab, and demonstrated the beauty of optimization modeling in pyomo. Luckny is a guru in stochastic programming and has always been the first reader of my manuscripts. I am grateful to his valuable comments as well as profound suggestion. Amandeep is the joy of the group, and never fails to propose fantastic restaurants and weekend activities. I enjoy every group outing organized by him. Jialin has such an easy-going personality. The small chats scattered within a hard-working day always make me more productive and positive. I wish I could be a lifelong friend with you all.

Furthermore, I would like to thank Debbie for her administrative support. She always takes care of anything, any questions, and any concerns. She is always there, friendly, smiley and ready to help. Always seeing her in the hallway, I took Riley Robb as my second home in the past five years.

Last but not least, I am blessed to have my endearing parents, Feiyue Cheng, and Wenjun Ba. They are with me in my darkest times, taking care of my emotional and life needs, listening to my complaints, and humoring my bursting of anger. They are always my harbor, my backbone, and my last resort. I would never be able to achieve this far without their support and encouragement.

CONTENTS

Biographical Sketch	iii
Dedication	iv
Acknowledgements	v
Contents	vii
List of Tables	ix
List of Figures	x
1 Introduction	1
1.1 Process Synthesis	3
1.2 Strategy Formulation	7
1.3 Organization of the Dissertation	10
2 Short-term Planning and Hedging for a Lignocellulosic Biorefinery under Carbon Constraints and Price Downside Risk	12
2.1 Introduction	12
2.2 Methodology	17
2.2.1 Case Study and Assumptions	17
2.2.2 Phase 1: Process Design and Production Planning	20
2.2.3 Phase 2: Managing Financial Risk during operation	25
2.2.4 Solution Procedure	28
2.3 Results	29
2.3.1 Production Commitment: The Influence of Carbon Tax	30
2.3.2 Refined Production Schedule and Hedging Strategy	32
2.4 Conclusions	39
3 Long-term Planning and Hedging for a Lignocellulosic Biorefinery under Carbon Constraints and Price Downside Risk	41
3.1 Introduction	41
3.2 Problem Statement and Assumptions	44
3.3 Model Development	45
3.3.1 A two-stage stochastic program	46
3.3.2 A long-term time series model for ethanol spot price	50
3.3.3 A simple pricing formula for ethanol swap contracts	51
3.4 Results	53
3.4.1 Results for Schwartz-Smith (SS) two-factor models	53
3.4.2 Production schedule and hedging decisions	54
3.4.3 Storage and selling decisions	58
3.4.4 Risk management with cVaR constraints	60
3.4.5 Sensitivity Analysis	61
3.5 Conclusion	65

4	Validation of the model framework in a first generation biorefinery	67
4.1	Introduction	67
4.2	Problem Statement and Assumptions	69
4.3	Model Development	71
4.3.1	A two-stage stochastic program	73
4.3.2	A bivariate time series model for corn and ethanol spot prices	77
4.3.3	A simple pricing formula for ethanol swap contracts	78
4.3.4	A backtesting model to compare the realized profit and the negotiated profit	80
4.4	Results	81
4.4.1	Results for vector error correction model	81
4.4.2	Production schedule and hedging decisions for risk neutral and risk averse producer	84
4.4.3	Backtesting results	87
4.5	Conclusion	90
5	Conclusion	92
	Bibliography	95

LIST OF TABLES

2.1	Conversion rate for each operating unit, based on [28]	18
2.2	Plant decision variables for simulated biorefinery	31
2.3	Production and financial strategy for the case 1 ($cVaR \geq 0$)	33
2.4	Different cVaR threshold versus objective values. Note that in- creasing K indicates higher risk aversion, and lower NPV	34
3.1	Nomenclature	47
3.2	Parameter values for the SS two-factor model.	53
3.3	Model selection criteria for two reference models	54
3.4	Case-Study Parameters for two-stage stochastic program	56
3.5	Expected profit and normalized standard deviation for decreas- ing risk levels	60
3.6	Alternative spot price patterns, generated from historical data (weeks indicated)	62
3.7	Expected profit and normalized standard deviation for cases with different storage capacity, showing that higher storage ca- pacity leads to higher expectation and standard deviation of profit, at the same risk level.	64
4.1	Nomenclature	73
4.2	p value for the Engle-Granger test from 2009 to 2015	82
4.3	Model order from 2009 to 2015	82
4.4	Model parameters of Year 2009 and Year 2015	83
4.5	Case-Study Parameters for two-stage stochastic program	85
4.6	Expected profit and normalized standard deviation for risk neu- tral and risk averse operators	87

LIST OF FIGURES

2.1	Process Flow for Biochemical Conversion to Ethanol	17
2.2	A demonstration plot of unit carbon tax	19
2.3	Solution procedure	29
2.4	Production commitment against Region 3 unit carbon tax shows higher carbon taxes lead to lower production commitment	31
2.5	NPV distribution for case 1 $cVaR \geq 0$	32
2.6	NPV distribution for different $cVaR$ threshold, shows decreasing volatility with increasing $cVaR$ constraints	33
2.7	Production level in each month for different price pattern	35
2.8	Portion of ethanol sold in forward market in each month for different price pattern	35
2.9	Monthly production level with and without inventory, shows access to storage allows for high production level at low forward price month	37
2.10	Last month product selling and inventory portion, shows that portion sold on forward contracts (yellow) increases with increase risk aversion	38
2.11	NPV distribution for different cases	38
2.12	Impact of Inventory Costs on Storage Utilization	39
3.1	Bioethanol hedging using swap contracts	52
3.2	The sequence of the four swap contracts used in the model . . .	52
3.3	A Sample set of weekly ethanol spot price scenarios	55
3.4	weekly spot price and one-year ahead price forecast with error bars.	55
3.5	Weekly production levels corresponding to second region unit carbon taxes (k_2), with decreasing spot price trend, shows that increasing carbon tax leads to declining production.	57
3.6	Production and hedging level with storage	58
3.7	Production and hedging level with no storage capacity	58
3.8	Sales and storage behavior for high, medium, and low spot price trends: ethanol spot market sales (left panel) and storage level (right panel)	59
3.9	Shares of swap entered for decreasing risk levels	61
3.10	Production levels for alternative spot price trends	63
3.11	Hedging level for risk averse case and different storage capacities, note higher storage capacity leads to more storage in Q1, thus decreasing the shares of swap contracts used	64
4.1	Process flow for corn biorefinery	70
4.2	Bioethanol hedging using swap contracts	79
4.3	The sequence of the five swap contracts used in the model	79

4.4	Monte Carlo forecast benchmarked on the real spot price, the forecast year is 2010 and 2016.	83
4.5	Profit distribution and operation strategies for risk neutral and risk averse operators, $Q_{c/e}$ represents the quantities of corn/ethanol per week	86
4.6	Top figure: profit comparison, middle figure: production and product hedging decisions for risk averse operator, bottom figure: profit margin	89
4.7	Impact of changing the fixed rate prices on the profit difference, where the profit difference is defined as realized profit, \mathcal{P}_t , less the negotiated profit, \overline{Pr}	90

CHAPTER 1

INTRODUCTION

Renewable energy production has increased significantly during the recent decades. Gelman [13] indicates that the installed global renewable electricity capacity nearly doubled between 2000 and 2011. In the United States, renewable energy accounted for 11.7% of the energy production in 2011, and more than half of this is provided by biofuels. The reason for biofuel's popularity is twofold: first, it is compatible with the supply chain of the crude-based fuels, and second, current automobiles can use a blend of bio- and crude-based fuels with few changes in their design.

The production of biofuels and bioproducts is based on a process encompassing a wide range of technologies to separate biomass into their building blocks, such as carbohydrates and proteins (further details in 1.1). These building blocks can then be converted to a fuel product like ethanol, butanol, and other industrial chemicals. The evolution of the production process has gone through three generations. The first generation of biofuel produces ethanol from corn and sugarcane, and has been the primary source of ethanol production in the US. However, there are several ethical problems related to the use of food crops as the raw material as well as the competition for the land use devoted to producing these food crops. In an effort to mitigate these concerns, the second and the third generation biorefineries have been developed to produce bioethanol from lignocellulosics such as grasses, woody crops, and agriculture residues, and algae respectively. While the second and third generations are believed to have potential, they currently face challenges in financial sustainability. To date, the crash of KiOR [17] as well as the bankruptcy of VeraSun

Energy [41] are among the most recent examples of failure that are shedding doubt on the financial viability of these more advanced biofuel processes.

To cope with the aforementioned economic feasibility issues, process system engineering emerges as one promising method that investigates the integration and use of various technologies to maximize the process profit. In the recent decades, two types of the methods have been specifically considered:

1. Process synthesis: for a specific type of process, choosing the optimal technology among several alternatives so that the whole process attains the optimal objectives, which ranges from economic, environmental, to social benefit.
2. Strategy formulation: for a given process with fixed operating units, exploring the methodology of financial risk management, which includes effective production scheduling, product price determination, and using financial derivatives.

While process synthesis is especially effective in determining the optimal units for a specific process, for a fixed process with given operating units, strategy formulation aims at formulating operational and risk management strategies to maximize the process profit.

Since the goal for this work is to propose operational and risk management strategies for a second generation biochemical biorefinery with predetermined operating units, an algorithmic framework is developed to output the optimal production and hedging decisions under a combination of process, financial, and environmental constraints. To further validate the proposed methodology framework, the method is back tested on a first generation biorefinery with the

historical price data. It is the hope that this work can provide a system of concrete and feasible solutions for both the first and second generation biorefinery operators to manage their price risk and maximize the facility's profit.

The rest of this chapter presents some literature survey on both the process synthesis and strategy formulation. Finally, the organization of the rest of the dissertation is presented at the end of the section.

1.1 Process Synthesis

Process synthesis is defined as choosing a combination of operating units among several alternatives to maximize a specific objective. A typical second-generation bioethanol production process includes: pretreatment, conversion and purification. There are several candidate technologies available to fulfill each step [37]. Major pretreatment methods include physical pretreatment like grinding, milling or chipping, physicochemical pretreatment like steam explosion, ammonia fiber explosion (AFEX), chemical pretreatment and biological pretreatment [36]. Via pretreatment, the physical structure of the feedstock has been decomposed, which liberates hemicellulose and cellulose from the matrix of the feedstock. The exposed hemicellulose and cellulose then proceeds through the conversion step. In the conversion stage, there are three types of methods, namely hydrolysis and fermentation, gasification, and pyrolysis.

Enzymatic hydrolysis of the hemicellulose and cellulose takes place in stirred tank reactors during which hemicellulose and cellulose are broken into fermentable sugars [48, 25, 65, 23, 61]. Next, the sugars, mainly glucose and xylose, are fermented into ethanol. A number of different products are obtained

together with ethanol, such as acid products from the metabolic paths of the microorganisms [48, 65, 61].

As for gasification [35], the first step includes two alternatives, indirect low pressure gasification with steam and direct high pressure gasification with steam and oxygen. The second step comprises technologies to remove solids and other compounds, such as hydrocarbons, ammonia, carbon dioxide, and hydrogen sulfide, to achieve the desired gas composition. Finally, two conversion alternatives are considered. The first option is the fermentation path where the syngas is fermented to ethanol in a stirred tank reactor. The second path is the high alcohols synthesis production [47]. In this path, the syngas is converted to the alcohol mixture across a fixed bed catalyst. After alcohol synthesis, the liquid alcohols are sent to the separation and purification units while the residual gas stream is recycled back to the reactor.

Pyrolysis is the thermal degradation of biomass by heat in the absence of oxygen, which results in the production of charcoal (solid), bio-oil (liquid), and gaseous fuel products. Depending on the operating conditions, the pyrolysis can be divided into three subclasses: (a) conventional pyrolysis, (b) fast pyrolysis, and (c) flash pyrolysis [64]. In this study, the biorefinery using the enzymatic hydrolysis path is considered as it requires only few changes to the process design of first generation biorefinery and is the most common second generation process configuration in the US.

In addition to the process specifics, it is likely that biorefinery processes, along with most industrial production facilities, will deal with new policy resulting from climate-change mitigation efforts. With a growing consensus that carbon emission, if left unchecked, will lead to major changes in the climate

system, governments are under growing pressure to enact legislation to curb carbon emissions [4]. The primary forms of carbon regulation include carbon taxes, a strict emission cap, cap and offset, as well as cap and trade. Entities such as European Union, United States, Australia, and New Zealand are or previously collected carbon taxes whereas other countries like China and Japan are moving in this direction. Biorefineries worldwide will need to adjust their production decisions in response to any changes in carbon emission policy. In any work considering the viability of a biofuel product, possible policy impacts should also be included. In the following paragraphs, papers addressing the process synthesis and environmental policy are summarized.

Zondervan et al. [66] have established a biorefinery optimization model for a multi-product system. They consider a production network of 72 processing steps that can be used to process two different feedstocks and produce four types of products. Martin et al. [35, 36, 37] have formulated energy-optimized biorefinery conceptual models via hydrolysis and gasification of switchgrass. They postulate a superstructure that contains multiple candidate technologies in each conversion step, and formulate a mixed integer nonlinear program to solve for the optimal configuration after considering both heat and water integration. Ponce-Ortega et al. [49] have proposed a disjunctive programming approach to identify the optimal biorefinery configuration for a given criterion (for example the economic, environmental, or safety, etc). The proposed approach enables the user to solve a difficult problem through a set of easy subproblems. Ng et al. [58] have adapted a fuzzy mathematical programming approach to synthesize a sustainable integrated biorefinery that fulfills both economical and environmental considerations. Romagnoli et al. [20] developed a strategic and operational decision framework by exploiting the advantages of process sim-

ulation and hybrid optimization. Furthermore, they also fully explore the inherent nonlinearity in the conversion mechanisms of a integrated biorefinery by incorporating the kinetics of complex biological reactions in the process simulation. Floudas et al. [2] proposes the optimal configuration for a hardwood biomass to liquid transportation fuels process. The optimality of the solution is achieved through the use of piecewise linear underestimation of nonlinear terms and a rigorous global optimization branch-and-bound strategy. In this thesis, the nonlinear constraints are treated using the same fashion as Floudas et al. [2].

Motivated by the potential of reduced greenhouse gas emission from lignocellulosic biorefinery facility, early studies have focused on the evaluation of life cycle greenhouse gas emissions of a given facility. For example, Seabra et al. [42] conduct a life cycle analysis on a renewable jet fuel facility in Brazil with a consequential approach. They conclude that the major contributions to emission are feedstock production and land use change (LUC) impact. Studies such as Mullins et al. [43] also consider the uncertainty in the life-cycle analysis model. Monte Carlo simulation is applied to estimate the life cycle emission distribution of corn ethanol. They conclude the potential GHG emissions reduction from biofuel is hard to forecast given the high degree of uncertainty in the model. They further conclude that incorporating uncertainty into decision making process enables the illumination of risk of policy failure. Later studies also include financial analysis into environmental assessment. For instance, Pereira et al. [46] have formulated both deterministic and stochastic models to determine the financial viability of producing n-butanol through two different pathways. The results illustrate a promising revenue per tonne of sugarcane, but a discouraging internal rate of return. Moreover, Monte Carlo simula-

tion conducted in the stochastic model shows high risk in producing n-butanol from ethanol catalysis. Pereira et al. [45] also compare the economical viability of two competing process, the acetone-butanol-ethanol (ABE) fermentation and ethanol catalysis. The results show the acetone-butanol-ethanol (ABE) fermentation has stronger financial performance, and n-butanol demonstrates over 50% emission reduction.

1.2 Strategy Formulation

In addition to process synthesis, strategy formulation is the other promising method to enhance the process profitability. Instead of assuming a fixed feed-stock/product price, this method aims at finding the optimal operation and hedging strategies for an energy facility under price variations. Specifically, while the second generation biorefinery faces the price uncertainty from ethanol side, the first generation biorefinery encounters price risk from both corn and ethanol. An ethanol producer, if fully exposed to price variation, could suffer significant financial loss during drastic price fluctuations. Hence, the strategy to manage operator's risk can be categorized into two groups.

1. Flexible Production Schedule: operators determine their production level and selling quantity according to the price movement.
2. Hedging with Financial Derivatives: using financial derivatives to lock in the purchasing/selling price for corn/ethanol.

While the early studies have been mostly focused on analyzing the financial feasibility of operating a biorefinery, recent research has explored the topic of

strategy formulation.

On the financial feasibility side, earlier researchers have focused on finding the ethanol threshold prices of entering and exiting the business for a corn biorefinery under policy and supply-side price uncertainty [54, 53, 30, 38, 39, 34]. Schmit et al. [54] have determined the ethanol gross margin for different scales of corn ethanol plants under increasing price volatility. They further conclude that the ethanol margin variability delays the new plant investment and exiting of operating plants. In their later study [53], the recent US renewable energy policy change is investigated and its impact on the development of corn biorefinery is quantitatively measured. This line of inquiry concludes that the existence of this policy has ensured the survival of the plants, and has narrowed the distance between optimal entry and exit curves. The work of Kirby et al. [30] uses Monte Carlo methods to assess the value of a corn ethanol facility under a real options framework, showing that even a modest increase in correlation between gasoline and corn prices significantly devalues the plant. Based on the Kirby et al. [30] work, Maxwell et al. [38] determine the managerial decision for a corn biorefinery to switch between operating and suspending the plant. The authors also demonstrate that increasing correlation between corn and ethanol prices is detrimental to the biorefineries, and without government subsidy, the plant is still profitable but embraces larger risk. Maxwell et al. [39] develop a quantitative framework to model and interpret regulatory changes during the life of a corn biorefinery, and concludes that the policy uncertainty may impact the plant's profitability either way depending on the subsidy level. And since the operator is risk averse, it is always optimal to switch off the plant before the policy changes. Finally, Li et al. [34] evaluates whether it is a good time to invest in cellulosic biorefinery in Iowa, and conclude that it is profitable yet

non-optimal to invest in pyrolysis-based biorefinery and the gain from waiting exceeds the costs of delaying the investment project.

On the strategy formulation side, in the pioneering work by Barbaro et al. [3], a two-stage programming methodology has been proposed and different risk measures such as downside risk, value-at-risk (VaR) and conditional value-at-risk (cVaR) are suggested. In their later study [50], the above framework is applied to a commercial petroleum refinery, Bangchack Petroleum Public Company Limited, to determine the crude oil purchase and production level under demand uncertainty. Results have shown the stochastic model outperforms the deterministic model in terms of expected profit and risk level. In some later studies, financial tools such as forward contracts and futures are incorporated to hedge the risk. For example, Park et al. [44] consider the financial risk management of a refinery via diversifying suppliers and futures contracts. Yun et al. [63] implement futures contracts to hedge against the fluctuating price pattern for raw materials, and create a model for multi-product biorefinery to enhance the process profitability. Recently, researchers also develop other methodologies to address the challenge in price risk. For example, Calfa et al. [7] develop an optimization framework to address both contract selection and price optimization with different price models. A deterministic optimization is implemented first, and then a stochastic model considers demand and raw material price uncertainty. In their later study of the optimal procurement process in an oil refinery [29], financial derivatives and production flexibility strategies have been introduced in a one stage stochastic programming framework. Cheali et al. [9] explore the effect of market price uncertainty on the design of optimal biorefinery configuration through a computer-aided decision support tool. Geraili et al. [21] add a downside risk measure to their previous decision framework [20]

to control the price uncertainty, which leads to a multiobjective optimization.

While the previous work discussed here have all contributed to the discussion of improved financial viability for the biorefinery, none considers the impact of environmental constraints on the operational and hedging decisions. Moreover, among the few studies modeling the use of financial derivatives and characterizing the price uncertainties, the models are oversimplified, thus fail to reflect the reality. To this end, the work presented herein seeks to address these issues through improved modeling of environmental constraints, as well as more detailed representation of financial derivatives for risk management. This dissertation considers three distinct scenarios, each in a stand-alone manuscript. First, a sequential stochastic programming model is created to determine the short-term production commitment and hedging decisions. The environmental constraints are considered by imposing tiered carbon tax constraints [11]. Second, long term production and hedging decisions have been formulated for under heavy carbon constraints. The long-term ethanol spot price uncertainty is modeled with a more sophisticated time series model [12]. The third and final study developed addresses similar questions, but is applied to the case study of a first-generation biorefinery, and backtested to approximate the lost revenue that the industry practitioners incur with the current operation practice.

1.3 Organization of the Dissertation

The dissertation is structured as follows:

Chapter 2: In this chapter, a model framework to determine the short-term production and hedging strategy is developed using two-phase stochastic pro-

gramming. The model takes into account the existence of carbon tax and explores the tradeoff between risk preference level and hedging decisions. Storage capability is also considered as an extra layer of profit protection. The material in this chapter appears as published in [11].

Chapter 3: A model framework to determine the long-term production and hedging strategy is developed. The development of the long-term strategy requires considerations of factors that were not required for the initial short-term implementation. Specifically, more advanced financial instruments are applied, with swap contracts providing more flexible hedging options. In addition, the longer-term models require a more refined time series model, which is provided by a two-factor time series model [55] that is better suited to this decision horizon. The factors that influence the production schedule are fully explored. The work of Chapter 3 also appears in the literature in [12].

Chapter 4: As the first generation biorefinery is still the dominant process producing bioethanol, the model framework proposed in Chapter 3 is applied to a case study of a first-generation biorefinery to validate the feasibility of proposed methodology. To fully consider the intricacy of the reality, both feedstock and product price uncertainties are considered by developing a bivariate time series model. The operating and hedging decisions obtained from the model framework are backtested using historic price data from 2010 to 2016. Finally, the resulting realized profits are compared with the “fixed” profits, which are derived from the current industry practice.

Chapter 5: The conclusions from all the previous three studies are summarized.

CHAPTER 2

SHORT-TERM PLANNING AND HEDGING FOR A LIGNOCELLULOSIC BIOREFINERY UNDER CARBON CONSTRAINTS AND PRICE DOWNSIDE RISK

This chapter proposes the use of forward contracts to mitigate risk. Moreover, it also considers the impact of carbon tax constraints and price uncertainty. Specifically, a stochastic optimization approach is implemented to develop strategies, which increases the net present value (NPV) of a production facility through determination of an optimal production schedule, as well as the creation of a portfolio of forward contracts to reduce product price risk. Results of numerical case studies show that if the policymaker is risk averse, production is higher in the early planning period rather than the later period. This chapter also investigates the ability to maintain inventory in order to create additional financial benefit¹.

2.1 Introduction

Production of fuel from biomass feedstock faces uncertainty in technology, logistics and market development, thus creating challenges for the industry investor [60]. Non-food feedstocks such as corn stover and perennial grasses have the most potential to be adopted in the future generation of biofuel facilities. In order to develop a viable biofuels industry, it is necessary to overcome challenges in process technology, and to determine optimal platform design. In addition, the financial viability of the process are sufficiently unstable that

¹©2016 Elsevier. With permission from my co-author: C. Lindsay Anderson. "Financial sustainability for a lignocellulosic biorefinery under carbon constraints and price downside risk." *Applied Energy*, 177:98–107, 2016.

investment in the industry will require succinct understanding of market dynamics, and careful management of financial risks. Financial derivatives, such as forward and swap contracts are widely used in the energy industry to hedge against the price downside risk [18]. Moreover, the price of biofuel based energy products does not take into account the cost of greenhouse gas emissions resulting from their production [62]. National governments can play a role in accomplishing a deduction of greenhouse gas emission by imposing carbon emission tax [59], thereby increasing the production cost of a biorefinery. According to Boldrin et al. [6], although a biorefinery is generally recognized as a tax credit earning facility thanks to its greenhouse gas emission reduction, this is not universally true due to the choice of calculation criteria. As a result, it is necessary to consider the production schedule under stringent carbon tax policy.

The main purpose of this study is to determine an optimal production schedule and ethanol forward contract strategy for a biochemical lignocellulosic biorefinery, in order to maximize its net present value under an acceptable level of risk. Throughout this study, the process model developed in Humbird et al. [28] is used. In addition, the forward contracts are assumed to be readily available between the biorefinery and its counter-party. The forward contracts' strike prices are determined empirically through historical spot price average. The contract pricing problem is not addressed in this paper, but is discussed in the future work.

As a summary, the current study contributes to the state of the art by considering the following aspects:

- This study considers the impact of environmental constraints on the financial sustainability of the modeled biorefinery. The proposed model in-

cludes a tiered carbon tax constraint, determining the optimal production commitment over the planning horizon.

- This study bridges the gap between sophisticated process design and simplified market financial risk management by striving for a balance. On the process design side, we model a lignocellulosic biorefinery from Humbird et al. [28] and obtain the optimal production commitment. On the risk management side, both endogenous (production scheduling) and exogenous methods (building a forward contract portfolio) have been considered. Moreover, the proposed exogenous risk management methods are highly related to the lignocellulosic biorefinery industry due to its primary focus on product side risk.
- To our knowledge, none of the reviewed literature considers the impact of inventory cost on facility's profit. The unit inventory cost is investigated in this work and the threshold value, after which the inventory policy becomes unfavorable, is assessed.

The chapter is organized as follows. Section 2.2 includes the description of the process parameters and assumptions, the formulation of the optimization model, and the solution procedure. The results are discussed in Section 2.3. Finally, in Section 2.4 the conclusions are drawn.

Nomenclature

Sets

i	chemical components
j	operating unit
r	unit carbon tax price regions
l	ethanol spot price scenario index
q	month index

Parameters

M_i	molecular weight of chemical component i
Φ_i	composition of chemical component i in feedstock
T_j	required temperature in operating unit j
Cp_i	heat capacity of chemical component i
$Price_i$	price of chemical component i
H_i	enthalpy of chemical component i
$Purindex_j$	purchasing cost index for operating unit j
a_j	installing cost multiplier for operating unit j
b_j	base price for operating unit j
$ratio_r$	upper bound ratio of greenhouse gas emission for Region r
$unit_r$	unit carbon tax price for Region r
FOC_r	process fixed operating cost corresponding to Region r
\underline{fs}	lower bound of the feedstock's hourly availability
cap	production capacity of the process
$Boil$	boiler efficiency
$Turbo$	Turbo generator efficiency
η	electricity surplus ratio
Tax	tax rate
IRR	internal return rate
$Time$	process lifetime
K	user defined lower bound for NPV
F_q	Forward contract price for month q
$P_{l,q}$	ethanol spot price for month q and scenario l
$P_{ethanol}$	ethanol historical mean spot price
$cost$	unit inventory cost
\bar{S}	lower bound for ethanol spot price of the future month
\underline{S}	upper bound for ethanol spot price of the future month

Variables

First stage variables

Binary variables

y_r	indicator variable, carbon emissions in region r
-------	--

Continuous variables

Mass balance variables:

$f_{i,j}$	flow of chemical component i to operating unit j
$totalC$	total amount of organic compound discharged to water

Nomenclature Cont'd

<i>biogas</i>	total amount of biogas generated for electricity generation
<i>genCH₄</i>	total amount of CH ₄ generated
<i>genCO₂</i>	total amount of CO ₂ generated
<i>genNO_x</i>	total amount of NO _x generated
<i>fs</i>	feedstock used
<i>prod</i>	the amount of ethanol produced
<i>GHG</i>	total amount of Greenhouse gas produced

Energy balance variables:

<i>Q_{h_j}</i>	energy needed to heat the operating unit j
<i>Q_{c_j}</i>	energy produced from operating unit j
<i>Q_{fc}</i>	energy produced from cooling the final product

Utility variables:

<i>HP</i>	High pressure steam required for heating
<i>LP</i>	Low pressure steam required for heating
<i>CW</i>	Cold water required for cooling
<i>electricity</i>	total amount of electricity generated
<i>steam</i>	total steam generated

Cost variables:

<i>sales</i>	revenue earned from ethanol and surplus electricity
<i>VOC</i>	variable operating cost
<i>FCC</i>	fixed capital cost
<i>WC</i>	working capital
<i>IC</i>	equipment installing cost
<i>PC</i>	equipment purchasing cost
<i>TDC</i>	total direct capital
<i>TIC</i>	total indirect capital
<i>NI</i>	annual netincome for the plant
<i>NPV</i>	net present value

Second stage variables

Continuous Variables

<i>x_q</i>	Production level for month q
<i>w_q</i>	the amount of ethanol sold in forward market for month q
<i>c_q</i>	the amount of ethanol sold in spot market for month q
<i>I_q</i>	inventory levels for month q
<i>carbon_tax_{l,q}</i>	carbon tax collected for month q and scenario l
<i>revenue_l</i>	quarterly revenue for scenario l
<i>NI_l</i>	quarterly netincome for scenario l
<i>NPV_l</i>	net present value for each scenario
<i>α</i>	value at risk
<i>z_l</i>	an auxilliary variable defined in cVaR constraint

2.2 Methodology

2.2.1 Case Study and Assumptions

A biochemical conversion process typically consists of feedstock storage and handling, dilute acid pretreatment, saccharification and fermentation, product, water, and solid recovery. A schematic process diagram is shown in Figure 2.1. The biorefinery facility considered has an operating capacity of processing 84 tons of feedstock hourly and producing 20 tons of ethanol hourly. The process yield assumption are summarized in Table 2.1, based on studies of Humbird et al. [28].

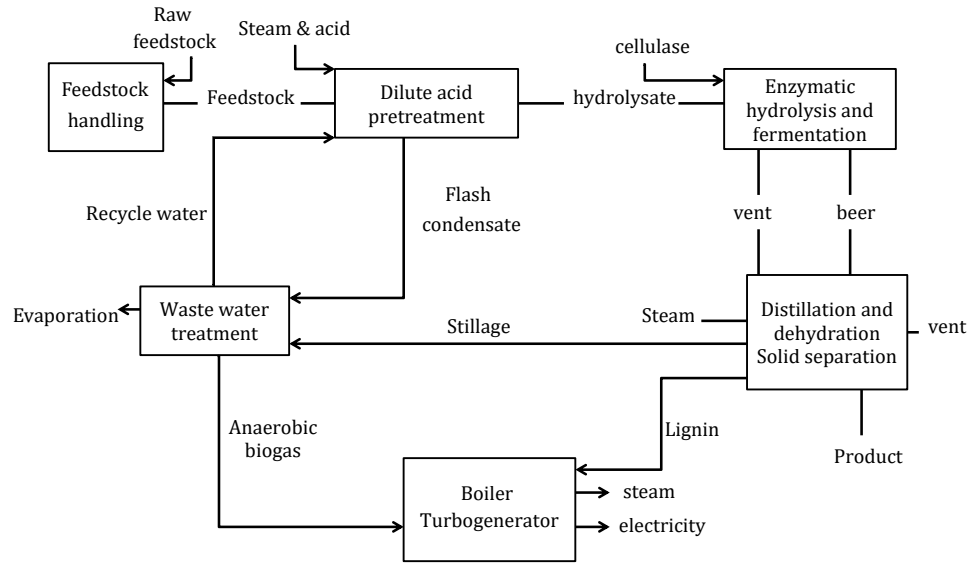


Figure 2.1: Process Flow for Biochemical Conversion to Ethanol

In line with the assumption in Humbird et al. [28], our research also assumes the greenhouse gas will be directly emitted and the energy collected from various operating units will heat process water to low pressure and high pressure

Table 2.1: Conversion rate for each operating unit, based on [28]

Pretreatment	9.9% cellulose → glucose 90% hemicellulose → xylose
Hydrolysis	91.2% cellulose → glucose
Fermentation	90% organic products remain 90% remaining glucose → ethanol 80% remaining xylose → ethanol
Waste water treatment	86% organic waste → biogas
Separation	85% anhydrous ethanol is obtained and the rest is recycled

steam for electricity generation.

In addition to the usual material, energy, capacity and financial constraints, this paper also assumes the existence of carbon tax. Specifically, the carbon tax policy is inspired by Chen et al. [10] which explores the impact of various carbon tax levels on production and profit scales at a bioprocessing facility. In this work a multi-echelon model is proposed, modeled on Benjaafar et al. [4] wherein the total carbon tax increases in a piecewise linear fashion as a function of the emission level, although other convex carbon tax policies are possible. This type of policy is illustrated in Figure 2.2

Note that the carbon tax region is defined by the ratio of the per unit carbon emissions and the total capacity of the process, as described in equation 2.1.

$$ratio_r = \frac{GHG}{Cap} \quad (2.1)$$

Given the process model and carbon tax policy summarized in Section 2.2.1, this paper considers the optimal production commitment for a quarter. Once the production commitment is determined, the operator faces the problem of

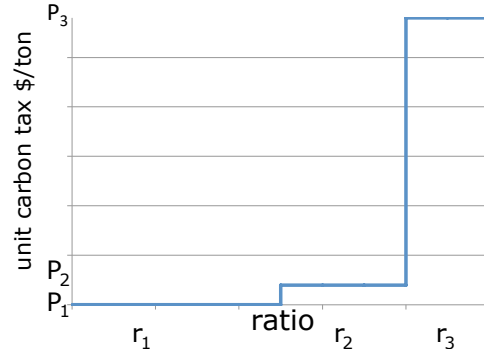


Figure 2.2: A demonstration plot of unit carbon tax

making scheduling decisions for each month within the longer planning horizon, and encounters product price downside risk. To hedge the price downside risks, a portfolio of forward contracts is built. When modeling the above decision timeline, a stochastic program with two sequential phases can be formulated, in which longer term planning commitments (*prod*) are made in the first phase, and a refinement of these decisions through determination of production scheduling (x_q) and forward contract portfolio (w_q) are established in the second phase.

These two phases are further elaborated in Section 2.2.2 and Section 2.2.3 respectively.

2.2.2 Phase 1: Process Design and Production Planning

As previously described, the goal of the first stage model is the overall optimization of the form in Equation 2.2:

$$\begin{aligned}
 & \max_x NPV \\
 & \text{subject to} \\
 & f(x) = b \\
 & g(x) \leq 0 \\
 & x \geq 0
 \end{aligned} \tag{2.2}$$

where the constraints for mass, energy, capacity, feedstock availability, emissions, utility and costs are given in (2.3)-(2.29). The process constraints include the mass and energy balances across all units, as well as feedstock requirements, and capacity limitations. Mass and energy balance constraints are given in (2.3)-(2.7), in which $f_{i,j}$ represents the mass flow of chemical component i in operating unit j , and Q_{h_j} , Q_{c_j} represent the heat generated/absorbed in the operating unit j . Equation 2.3-2.5 represent the material conservation for inert components, reactants and products respectively.

$$f_{i,j} = f_{i,j+1} \quad \forall i \in \text{inert} \tag{2.3}$$

$$f_{i,j} = f_{i,j+1}(1 - \text{conv_rate}) \quad \forall i \in \text{reactants} \tag{2.4}$$

$$f_{i,j} = f_{i,j+1} \cdot \text{conv_rate} \quad \forall i \in \text{products} \tag{2.5}$$

$$Q_{h_j} = \sum_i f_{i,j} C p_i (T_j - T_{j-1}) \tag{2.6}$$

$$Q_{c_j} = \sum_i f_{i,j} C p_i (T_{j+1} - T_j) \tag{2.7}$$

The capacity and feedstock constraints are given in equations (2.8) and (2.9), in which f_s should not exceed the upper bound of feedstock and the production

should not drop below the lower bound:

$$f_s \geq \underline{f_s} \quad (2.8)$$

$$prod \leq cap \quad (2.9)$$

Combustible organic byproducts separated from the process are fed to the combustor, boiler and turbogenerator system to produce steam and electricity. This allows the plant to minimize energy costs, as well as providing additional revenues through generation of surplus electricity to grid. Both high pressure and low pressure steam are produced during the process to fulfill heating requirement of other operating units. Moreover, cooling water is needed to condense the remaining steam and cool down the outlet streams in some operating units. Utility constraints are summarized below in equations (2.10)-(2.14). Specifically, Equation 2.10 calculates the amount of high pressure steam (*HP*) required to heat the dilute acid pretreatment and distillation step. Equation 2.11 represents the amount of low pressure steam (*LP*) consumed to heat the boiler. Equation 2.12 illustrates the cold water (*CW*) needed for outlet steam condensation, required for many of the operating units in this process. Equation 2.13 shows the amount of the steam (*steam*) generated from the boiler equals to the total heat released from burning organic waste (mainly methane and lignin) divided by the specific enthalpy change of water. Finally, Equation 2.14 calculates the total watts of electricity (*electricity*) which comes from converting the heat

of surplus steam in turbogenerator.

$$HP = \frac{\sum_{j=1,4} Q_{h_j}}{\Delta h_{high}} \quad (2.10)$$

$$LP = \frac{\sum_{j=5} Q_{h_j}}{\Delta h_{low}} \quad (2.11)$$

$$CW = \frac{\sum_{j=1,3,4,5,6} Q_{c_j} + Q_{fc}}{Cp_{i=H_2O}(100 - T_{amb}) + \Delta h_{water}} \quad (2.12)$$

$$\begin{aligned} steam = & \frac{Boil \cdot (genCH_4 \cdot H_{i=CH_4} + f_{i=lignin,j=3} \cdot H_{i=lignin})}{\Delta h} \\ & + \frac{Boil \cdot (f_{i=cellu,j=3} \cdot H_{i=cellu} + f_{i=hcellu,j=3} \cdot H_{i=hcellu})}{\Delta h} \end{aligned} \quad (2.13)$$

$$electricity = \Delta H_{specific} \cdot (steam - HP - LP) \cdot Turbo \quad (2.14)$$

Two sources contribute to the greenhouse gas emissions of the process, first fermentation ($f_{i=CO_2,j=3}$) and afterwards within the waste water treatment, where anaerobic digestion of the organic waste ($genCO_2$) occurs.

$$GHG = genCO_2 + f_{i=CO_2,j=3} \quad (2.15)$$

To address environmental concerns, a stepwise unit carbon tax policy is used, as described in Section 2.2.1. Therefore, a set of binary variables (y_r) is introduced to represent the carbon tax operating region decision. The upper bound for each region ($ratio_r$, see Equation (2.1)) is defined as the ratio of the greenhouse gas emission level to the total plant production capacity. Equation 2.16 represents the exclusive choice of a certain emission region the biorefinery operates on. Equation 2.17 calculates the total amount of greenhouse gas emission (GHG) based on the greenhouse gas emission region (GHG_r) the facility operates on. Finally, Equation 2.18 regulates the upper and lower bound

emission level at region r .

$$\sum_{r=1}^3 y_r = 1 \quad (2.16)$$

$$\sum_{r=1}^3 GHG_r y_r = GHG \quad (2.17)$$

$$cap \cdot ratio_{r-1} \leq GHG_r \leq cap \cdot ratio_r \quad (2.18)$$

Corresponding to the stepwise unit carbon tax and capacity level, total carbon tax (*carbon_tax*) and fixed operating cost (*FOC*) are calculated as piecewise linear functions (see Equation 2.19 and Equation 2.20). As a result, whichever region r is selected, the total carbon tax is the sum of the tax paid for all the former regions and the surplus amount of the current region.

$$carbon_tax = \sum_{i=1}^{r-1} cap \cdot ratio_i \cdot unit_i + (GHG - cap \cdot ratio_{r-1}) unit_r y_r \quad (2.19)$$

FOC_r is the base fixed operating cost for each capacity level, while variable operating cost (*VOC*) is the summation of all the raw chemical components used in the process.

$$FOC = \sum_{r=1}^3 FOC_r y_r \quad (2.20)$$

$$VOC = \sum_i Price_i f_{i,j=1} \quad \forall i \in raw\ chemicals \quad (2.21)$$

Capital costs are defined below. Both purchasing capital (*PC*) and installing capital (*IC*) are proportional to the material flow level in each operating unit (Equation 2.22 and 2.23), and other capital costs, such as total direct cost (*TDC*) total indirect cost (*TIC*) fixed capital cost (*FCC*) and working capital (*WC*) are

a function of installation costs (IC) extracted from [28] as (2.24)-(2.27).

$$PC = \sum_j \text{Purindex}_j \left(\frac{\sum_i f_{i,j}}{b_j} \right)^{0.7} \quad (2.22)$$

$$IC = \sum_j a_j \text{Purindex}_j \left(\frac{\sum_i f_{i,j}}{b_j} \right)^{0.7} \quad (2.23)$$

$$TDC = 0.175ISBL + IC \quad (2.24)$$

$$TIC = 0.6TDC \quad (2.25)$$

$$FCC = TDC + TIC \quad (2.26)$$

$$WC = 0.1FCC \quad (2.27)$$

Finally, profit related variables include sales, net income and net present value, among which maximizing net present value is the system objective. Sales ($sales$) are the summation of revenue from selling ethanol and electricity. Net income (NI) are defined as the sales net carbon tax, fixed operating cost and variable operating cost. Finally, net present value (NPV) is defined as the summation of the present value of net income after tax and depreciation subtract fixed capital cost and working capital.

$$sales = P_{ethanol} \cdot prod + Price_{electricity} \cdot \eta \cdot electricity \quad (2.28)$$

$$NI = sales - carbon_tax - FOC - VOC \quad (2.29)$$

$$\begin{aligned} \max NPV = & \sum_{l=1}^{time} \frac{NI(1 - tax)}{(1 + IRR)^l} - FCC \\ & - WC + \sum_{l=1}^{time} \frac{(FCC + WC) \cdot tax}{time \cdot (1 + IRR)^l} \end{aligned} \quad (2.30)$$

The first phase process model calculates the quarterly production commitment under carbon tax constraints, while the second phase financial risk man-

agement model is presented in the next section, representing a refined decision of production commitment.

2.2.3 Phase 2: Managing Financial Risk during operation

In the second phase, a stochastic program is formulated with the ethanol spot price as the source of uncertainty. Sample average approximation (SAA) [57] is applied to generate the deterministic equivalent of such a stochastic problem. Despite some drawbacks, GBM is widely used in mathematical finance and financial economics due to its simplicity and robustness for modeling financial time series [38]. In order to ensure that the uncertainty is sufficiently characterized, ten thousand ethanol spot price scenarios are generated from the GBM model, which is estimated using Iowa ethanol spot price data from year 2006 to 2014 [1].

Production scheduling

We initially consider the problem of production scheduling of each month to fulfill the commitment over the entire quarter. Therefore, the first constraint is to fulfill the production commitment,

$$\sum_{q=1}^T x_q = prod \quad (2.31)$$

while ensuring that the production level for each month should still satisfy the box constraint.

$$0 \leq x_q \leq cap \quad (2.32)$$

After fulfilling the production scheduling constraints, forward contracts decisions are introduced to hedge the product price downside risk.

Forward contracts

In the financial industry, a forward contract is a non-standardized contract between two parties to buy or to sell an asset at a specified future time at a price agreed upon today [27]. Forwards, like other derivative securities, can be used to hedge risk. For this reason, ethanol produced each month (x_q) is sold via a combination of spot market (c_q) and forward contracts (w_q):

$$c_q + w_q = x_q \quad \forall q \in 1, \dots, T \quad (2.33)$$

Corresponding to the use of forward contracts, the revenue, net income and net present value under each scenario l can be redefined as follows.

$$revenue_l = \sum_{q=1}^T F_q w_q + P_{l,q} c_q \quad (2.34)$$

where the F_q represents the forward price in each month, and $P_{l,q}$ represents the ethanol spot price in each month and scenario. The net income becomes

$$NI_l = revenue_l - VOC - FOC \quad (2.35)$$

And NPV under each scenario follows by summing the net income minus capital cost plus depreciation for all the periods.

$$\begin{aligned} NPV_l = & \sum_{t=1}^{time} \frac{netincome_l(1 - tax)}{(1 + IRR)^t} - FCC \\ & - WC + \sum_{t=1}^{time} \frac{(FCC + WC)tax}{time(1 + IRR)^t} \end{aligned} \quad (2.36)$$

Metrics for Risk Management

In the area of production economics, risk is generally defined as the potential loss due to the unexpected downfall of the product's price. Correspondingly, the risk preference is regarded as the maximum/minimum level of loss/profit the operator is willing to take when facing the price uncertainty. In the stochastic programming model, a single objective function of expected net present value is optimized. The solutions obtained are optimal on average, but risk preferences of the operators have not been considered. To explore the trade-off between different risk preference levels and optimal expected net present values, cVaR proposed by Rockafellar et al. [51] is used as a risk metric.

Conditional value at risk (cVaR) can be regarded as the average of some percentage of the worst-case profit scenarios [52]. We choose cVaR as our risk metric as it is a coherent risk measure and can be optimized as well as constrained with convex programming methods. A given quantile $\beta \in (0, 1)$ is considered along with two variables, value at risk (α) and deviation (z_l) between VaR and scenario net present value. If the net present value is less than α , z_l should be enforced to zero. The above relations can be included via the following constraints.

$$z_l < 0 \quad (2.37)$$

$$-\alpha + z_l + NPV_l < 0 \quad (2.38)$$

$$\alpha + \frac{1}{(1 - \beta)L} \sum_{l=1}^L z_l > K \quad (2.39)$$

With each of these components incorporated into the modeling framework, the model is solved by the solution procedure described in Section 2.2.4.

2.2.4 Solution Procedure

The overall model is comprised of first a mixed integer nonlinear program and second a stochastic linear program. Solving two phases together can be both computationally demanding and may not result in the global optimum due to computational limitations. To overcome these difficulties, the following procedure is proposed. The first phase mixed integer nonlinear program is solved with constraints (2.3)-(2.29) and objective function (2.30). To further increase the solution efficiency and ensure accuracy, the mixed integer nonlinear program is decomposed to three separate nonlinear programs and solved separately by a nonlinear optimization solver CONOPT. These three convex nonlinear programs represent the optimization of achievable net present value in the corresponding carbon emission regions, and the decomposition removed the dependence on binary variables. Once the emission region with optimal objective value is selected, corresponding decision values such as production commitment ($prod$), fixed operating cost (FOC), variable operating cost (VOC), and fixed capital cost (FCC) are input to the second phase, in which sample average approximation (SAA) method is implemented to discretize the stochastic program into the deterministic equivalent of linear program. The linear program is solved with constraints (2.31)-(2.35),(2.37)-(2.39) and objective function (2.36). This procedure is illustrated in Figure 2.3.

The computation studies were performed on a MacBook Pro Laptop with Intel(R) Core(TM) i7-3720QM, 2.60GHz CPU, and 8GB RAM. The model was coded in GAMS 24.1.1 and the first phase decomposed MINLP model was solved with the solver CONOPT, while the second phase LP model with CPLEX 12.5.0.1.

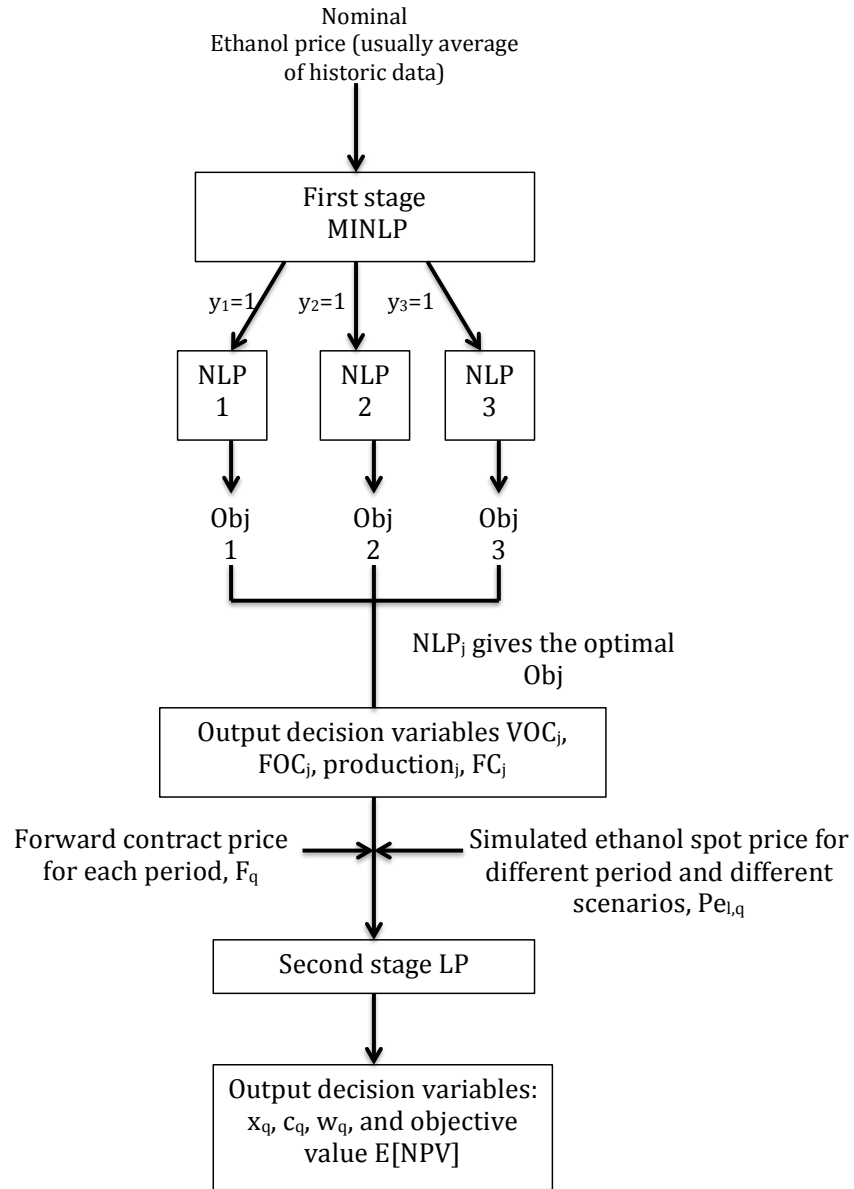


Figure 2.3: Solution procedure

2.3 Results

The goal of this approach is to develop recommendations for the production commitment, production schedule and hedging portfolio that minimize exposure to financial risk in the market. As previously described, the correlation

between carbon policy and production commitment is examined through the use of a tiered carbon tax function. Whereas the results of production schedule and hedging levels are affected by risk preference levels, spot price dynamics, forward price patterns and storage capacity. Three case studies have been performed to demonstrate these relationships. In the first case, a simple forward contract is applied with constant strike price throughout the planning horizon. While in the second case, forward contracts whose strike price varies monthly are considered. Finally, in the third case, storage capacity is added on top of time-varying forward contracts. To ensure a fair comparison on optimal expected NPV, risk preference levels are maintained within the three cases.

The first phase solution determines overall production commitment, byproduct credits and associated costs in Section 2.3.1. While the second phase decision determines the specific production schedule and hedging policy through three case studies in Section 2.3.2.

2.3.1 Production Commitment: The Influence of Carbon Tax

The first phase optimization model determines the most economically viable operating commitment for the simulated bioprocess facility, constrained by the overall production capacity, the greenhouse gas emissions, and production costs. Of primary importance is the determination of the impact of carbon policy on production commitments.

As shown in Figure 2.4 the economically efficient operating point is determined by the prices levels derived from the carbon tax policy. Once the operating regime is determined, it is always optimal to produce at the upper bound

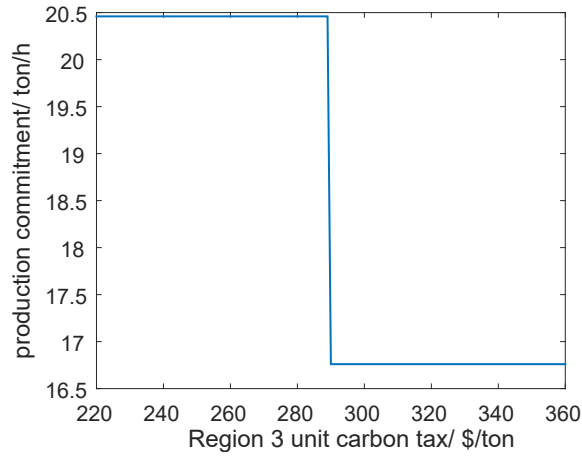


Figure 2.4: Production commitment against Region 3 unit carbon tax shows higher carbon taxes lead to lower production commitment

Production commitment	Costs
Production Level	16.76 ton/h
Electricity	0.6592 GJ/(ton ethanol)
VOC	3449 \$/h
FOC	869.1 \$/h

Table 2.2: Plant decision variables for simulated biorefinery

of the region. In addition, a high unit carbon tax (≥ 290 \$/ton) in Region 3 is prohibitive to full capacity production, driving a shift in operating levels from full capacity to some lower capacity level. Once the operating point is determined, the question of production scheduling and financial risk management can be addressed by the second phase optimization model. In order to examine the above two problems, we choose the unit carbon tax structure of 20\$/ton and 290\$/ton for regions 2 and 3, respectively, and the corresponding decision variables obtained from the first phase optimization are summarized in Table 2.2.

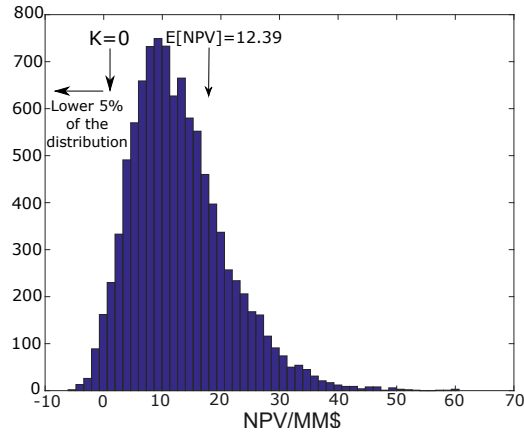


Figure 2.5: NPV distribution for case 1 $cVaR \geq 0$

2.3.2 Refined Production Schedule and Hedging Strategy

In the second phase, the operator will determine the optimal schedule and select a portfolio of forward contracts to manage the price risk for the ethanol product, based on ten thousand scenarios to represent the price uncertainty in the ethanol market.

First Case: Fixed Forward Prices

In the first case, we consider the most common approach wherein the highly risk-averse operator will seek to manage production and hedging decisions to avoid losses. This behavior is formulated by setting the $cVaR$ lower bound (K) to zero, which ensures that only the lower 5% tail of the NPV distribution is below zero. The results of the first case analysis are summarized in Figure 2.5 and in Table 2.3.

As shown in Table 2.3, a risk-averse producer will operate at full capacity in the first two months and sell most of the product in the forward market. It is

	First Month	Second Month	Third Month
production/ ton/h	13256.6	13256.6	9684.2
portion sold in forward contract market	0.336	0.336	0.218
portion sold in spot market	0	0	0.049

Table 2.3: Production and financial strategy for the case 1 ($cVaR \geq 0$)

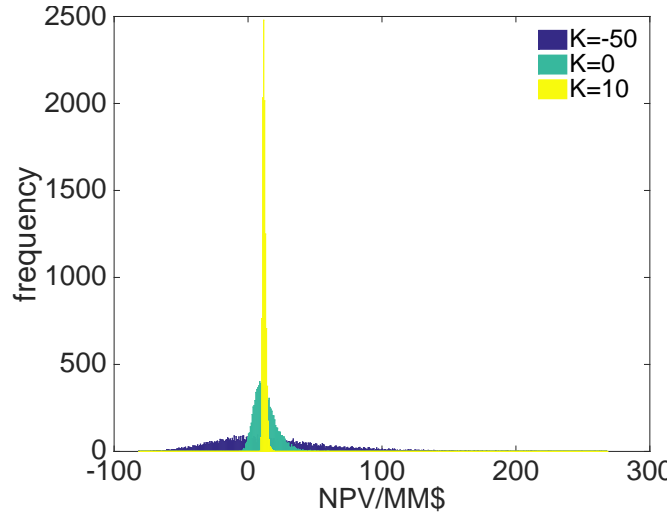


Figure 2.6: NPV distribution for different cVaR threshold, shows decreasing volatility with increasing cVaR constraints

also possible to reduce the risk of operations via manipulation of the cVaR lower bound (K), thereby reducing the variance of the NPV distribution as in Figure 2.6.

The model reduces the financial risk by increasing the portion of the product that is sold by the forward contract. This strategy reduces variability in product value and therefore, access to both downside and upside prices are limited. As a result, overall expected NPV decreases. This trade-off is illustrated in Table 2.4, which shows the expected NPV associated with various risk levels.

The results presented in the first case assume that forward prices are constant throughout the planning horizon of the facility. It is worthwhile to relax this

K/MM\$	E[NPV]/MM\$
-50	17.802
0	12.319
10	11.9569

Table 2.4: Different cVaR threshold versus objective values. Note that increasing K indicates higher risk aversion, and lower NPV

assumption and consider the impact of time-varying contract prices.

Second Case: Time Varying Contract Prices

In this context, three different contract price patterns are discussed, with the cVaR lower bound (K) set to zero to replicate the risk-averse decision maker.

- (a) $F_1 < F_2 < F_3$ (increasing)
- (b) $F_1 > F_2 > F_3$ (decreasing)
- (c) $F_1 > F_2 < F_3$ (valley)

Using these contract price patterns, the production schedules, and the hedging strategy are summarized in Figures 2.7, 2.8.

Examination of Figures 2.7 through 2.8 shows that the risk-averse decision maker allocates production corresponding to the forward price pattern. Production and sales are specifically maximized during the periods of highest forward prices. This allows the decision maker to simultaneously reduce risk with forward contracts, while maximizing the expected NPV of the facility.

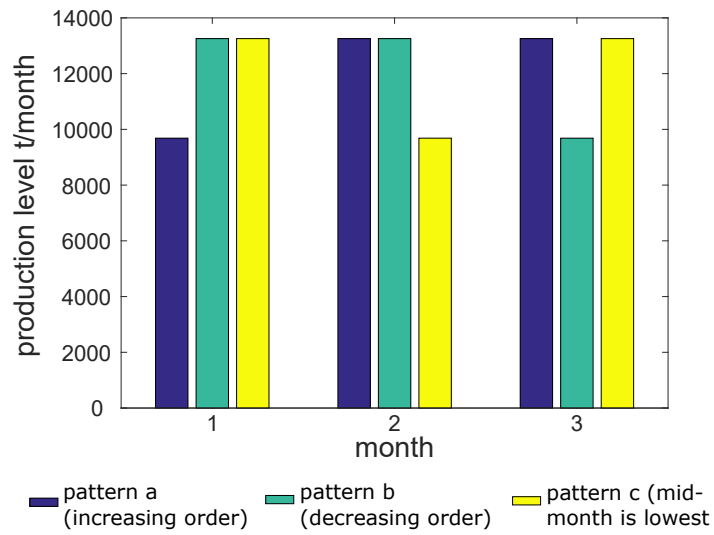


Figure 2.7: Production level in each month for different price pattern

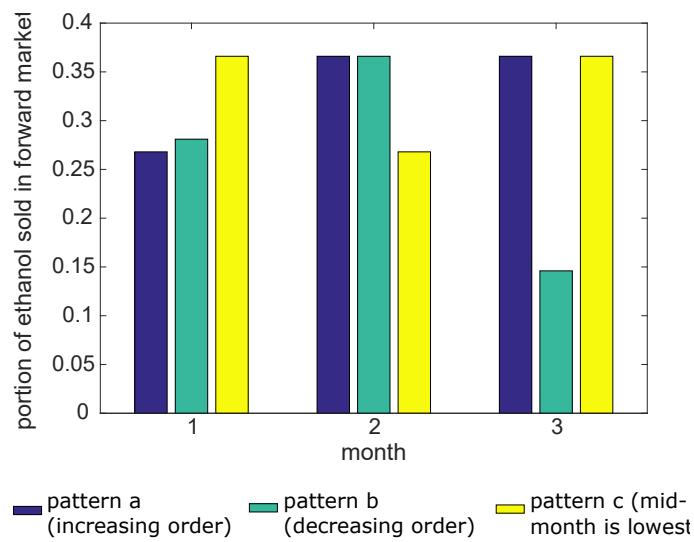


Figure 2.8: Portion of ethanol sold in forward market in each month for different price pattern

Third Case: Allowing Inventory

Another strategy for managing financial risk is the use of storage to provide flexibility to the decision maker. In the initial analysis, cost of inventory is neglected. Inventory existing at the end of the planning horizon is assumed to be sold on the spot market in the subsequent month, to minimize artificial boundary effects. Risk preference level is maintained ($K=0$) and the forward contract strike prices are time varying, following the increasing pattern as previously described.

Therefore, Equations (2.33),(2.35) are adapted to (2.40)-(2.43) to incorporate inventory.

$$c_q + w_q + I_q = x_q + I_{q-1} \quad \forall q \in 1, \dots, T \quad (2.40)$$

$$I_0 = 0 \quad (2.41)$$

$$NI_l = revenue_l + S_0 \cdot I_T - VOC - FOC - \sum_{q=1}^T I_q \cdot cost \quad (2.42)$$

$$S_0 \sim U(\underline{S}, \bar{S}) \quad (2.43)$$

Figure 2.9 compares monthly production schedule with and without inventory. The production schedule decisions under time varying forward contract price, with an increasing pattern, is used here. The reverse trend of production trend shows the ability to store enables high production at low forward price period. To consider the impact of risk preferences on storage behavior, Figure 2.10 demonstrates the relative portion of spot market sales (blue), forward market sales (yellow), and inventory in the final period (green), with respect to decreasing risk tolerance levels. As risk tolerance decreases, uncertainty is reduced by increasing sales via forward contract. Finally, the NPV distributions derived

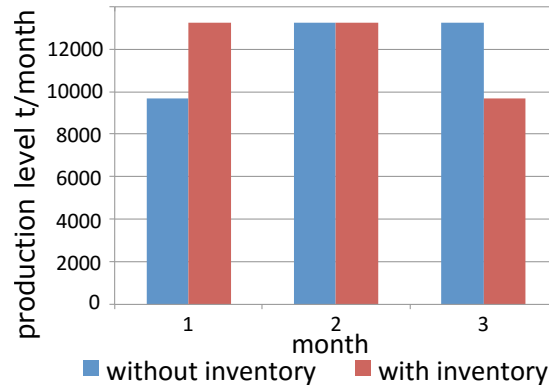


Figure 2.9: Monthly production level with and without inventory, shows access to storage allows for high production level at low forward price month

from the three cases are compared at the same risk preference level ($K=0$) as shown in Figure 2.11. The increasing instances in upper tail of the NPV distribution for Case 3 shows that inventory increases the likelihood of higher NPV, whereas fixed forward prices (Case 1) provide more NPV certainty with lower overall expected NPV.

Additional numerical tests support the fact that the three primary factors (forward prices, the risk preference level, and expected spot price in the future) jointly determine the inventory levels and portion sold on the spot market. While the above results only represent a policy under increasing forward price pattern and low risk preference level, various forward price and risk preference patterns can be implemented in order to generate corresponding decisions.

Finally, it is useful to consider the costs of inventory in a general way. Figure 2.12 shows the portion of product in inventory for each of the three months,

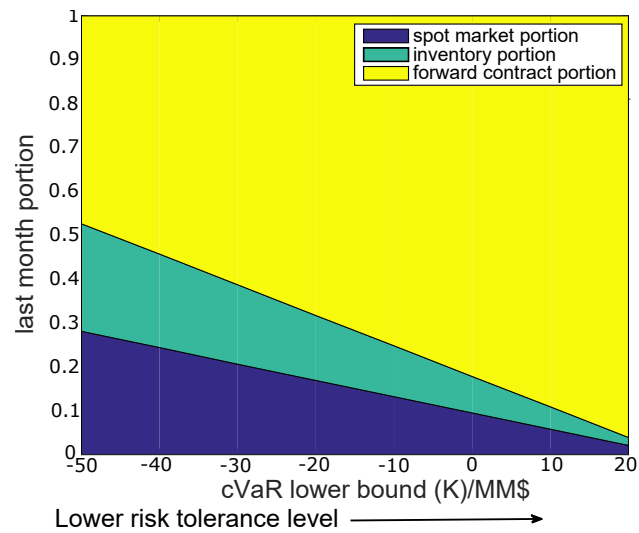


Figure 2.10: Last month product selling and inventory portion, shows that portion sold on forward contracts (yellow) increases with increase risk aversion

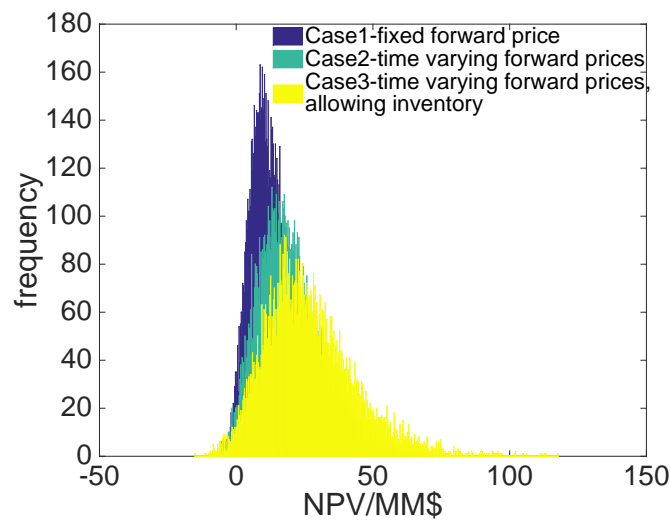


Figure 2.11: NPV distribution for different cases

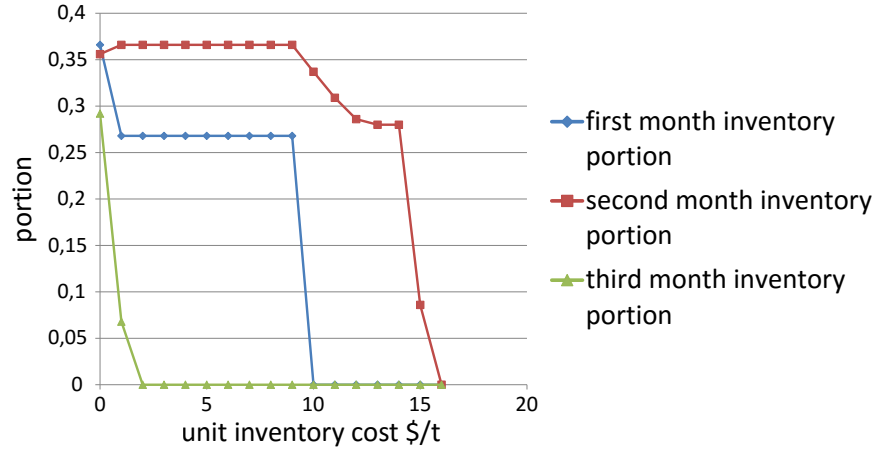


Figure 2.12: Impact of Inventory Costs on Storage Utilization

under a range of unit inventory costs.

The important aspect of this plot is the indication that inventory costs above the threshold values of 15\$/ton will negate any benefits of allowing storage. Typical storage costs for lignocellulosic feedstock are approximately 16\$/ton [14], which is likely to be higher than the cost of storing product due to lower bulk density. It is also worth noting that the usage pattern of inventory at each month is non-uniform due to the influence from the expected spot price in the future and product value at the end of the time horizon (S_0); thus, different inventory usage patterns would be obtained with alternative future spot price expectations.

2.4 Conclusions

This study has introduced a stochastic sequential programming approach to plan and schedule the production of a biochemical lignocellulosic biorefinery while managing financial risk that arises from price uncertainty. In the first

phase, the biorefinery is modeled under stepwise unit carbon tax constraints, based on the model introduced in [4]. First phase results indicate a move to lower production levels is caused by a prohibitively high carbon tax in Region 3 (≥ 290 \$/ton-unit).

Three cases have been considered in the second phase. In the first case, trade-off between risk and profit has been achieved by introducing forward contracts, which are effective tools in risk management. In the second case, it is shown that production and hedging policy correspond to forward price pattern in risk averse conditions. In the third case, it is demonstrated the ability to store will weaken correlation between production schedule and forward prices and will lead to a higher profit level. Whereas a unit inventory cost of 15 \$/ton will make the inventory strategy unappealing. Moreover, the use of storage and selling on the spot market decreases as the risk tolerance reduces, and the producer is driven to the price stability from forward contracts.

CHAPTER 3

**LONG-TERM PLANNING AND HEDGING FOR A LIGNOCELLULOSIC
BIOREFINERY UNDER CARBON CONSTRAINTS AND PRICE
DOWNSIDE RISK**

This chapter considers long-term production scheduling under the impact of carbon tax constraints and ethanol spot price uncertainty, as well as risk management via ethanol swap contracts. More specifically, a framework consisting of a two-stage stochastic program and a two-factor time series model is presented to determine the weekly production rate and swap portfolios to maximize the process profit under spot price uncertainty¹.

3.1 Introduction

Fuel production from biomass feedstock is hindered by uncertainties in process technology, logistics and market development. Non-food feedstocks such as corn stover and perennial grasses have the most potential to be adopted in future generation biofuel facilities. A recent report from Larsen et al. [32] suggests although the process is developed, and the products are on the market, further policy and market research are still imperative to ensure the construction of commercial plants. Therefore, both optimal conversion process design and financial risk management are essential to develop a commercially viable industry. Interviews with biorefinery operators have shown long-term production and risk management strategies are more favorable compared to the short-

¹©2016 Elsevier. With permission from my co-author: M. Gabriela Martinnd C. Lindsay Anderson. "Long term planning and hedging for a lignocellulosic biorefinery in a carbon constrained world." *Energy Conversion and Management*, 126:463–472, 2016.

term ones. As for the financial instruments used in risk management, swaps have gained substantial popularity in the last decade for long term risk management [18]. Therefore, it is essential to quantitatively model the use of swap contracts in long term risk management for biorefinery industry. Moreover, in most of the biorefinery process models, the environmental concerns, such as greenhouse gas (GHG) emission, are overlooked. According to Boldrin et al. [6], although a biorefinery is generally recognized as a tax credit earning facility thanks to its greenhouse gas emission reduction, this is not universally true due to the choice of calculation criteria in implementing life cycle analysis. As a result, it is necessary to consider the production strategy under a stringent carbon tax policy. Finally, unlike an ordinary oil refinery where the price uncertainty mainly arises from the supply side, the fair price of the feedstock of the second generation biorefinery is still in the exploration stage, therefore, no solid market has been formed to effectively manage the potential price uncertainty [33]. However, the price volatility for the final product can be a major concern.

As a result, this chapter contributes to the state of the art in the following directions:

- Related previous work such as Cheng and Anderson [11] or Ji et al. [29] assumes that the spot price follows Geometric Brownian Motion (GBM) , which is appropriate for shorter time horizons. Under a long-term horizon, the use of GBM to represent the underlying product price is no longer acceptable. The inherent drift in this type of model would result in more conservative production and hedging decisions for the biorefinery operator, thus leading to a suboptimal profit level. Therefore, for the longer term model developed here, a more realistic model is required. Specifically, a

sophisticated two-factor model is applied based on Schwartz et al. [55] to simulate the ethanol spot price and the fixed rate (formally introduced in Section 3.3.3) pricing of the swap contract.

- Previous research on the use of financial derivatives for risk management in this industry has focused on simple forward contracts. However, forward contracts are not frequently used in the commodity derivative industry, so this work extends the existing literature by considering the use of swap contracts for hedging.
- Compared with the previous studies invoking a real option approach to determine the projects' profitability and entry/exit threshold margin [54, 53, 30, 38, 39, 34], this study extends the richness and flexibility of operation and hedging decisions. Unlike the aforementioned works that address binary planning decision of switching on or off, this study also investigates the weekly optimal production level while adding hedging decisions as an extra layer of profit protection.
- Finally, in order to implement the improvements proposed above, and to account for influences between production, risk management, and storage decisions, the problem is solved in a two-stage stochastic optimization approach. This method, though more sophisticated than a sequential or single-stage optimization model, incorporates the appropriate time-sequence of production, storage, and sales decisions that will be made in practice.

The remainder of the chapter is organized as follows. Section 3.2 describes the problem in detail. In Section 3.3, the optimization model is formulated and time series model described. Results are provided and discussed in Section 3.4.

Finally, conclusions are delineated in Section 3.5.

3.2 Problem Statement and Assumptions

Given a lignocellulosic biorefinery facility exposed to two major external constraints; a specific carbon tax structure, and fluctuating ethanol spot price dynamics, the goal is to determine the long-term production and hedging strategies to maximize the facility's total profit and control the financial risk. The target biorefinery drawn from Humbird et al. [28] has the process flow diagram in Figure 2.1. The carbon tax structure described in Benjaafar et al. and Cheng et al. [4, 11] which increases marginal carbon tax with emissions level, is implemented. It is further assumed that there exist four swap contracts that mature quarterly. In this case, it is assumed maturity dates are in March, June, September and December, though these can be customized as necessary. The choice of four quarterly swap contracts matches with the long term hedging framework while ensuring the strategy flexibility. Although it is also possible to use swap contracts with longer tenor, such as one-year, this will result in a suboptimal profit level as the operator loses the flexibility to adjust the hedging decisions.

Such a strategic planning problem can be further decomposed into two sets of decisions, first the quarterly hedging level, the weekly production schedule over a year, and second, the weekly storage and selling decisions. The choice of hedging and production plan in an annual time frame corresponds with the goal of long-term planning, whereas weekly selling and storage decisions ensures the flexibility to adjust to different product price scenarios.

In the world of mathematical programming, such a problem can be formu-

lated as a two-stage stochastic program. Under the commonly acknowledged no-arbitrage financial assumption, long-term hedging (H_q) and production decisions ($prod_i$) need to be determined in the first stage before observing any spot price information ($spot_{i,j}$), whereas quick responses, such as selling ($Sa_{i,j}$) and storage policy ($St_{i,j}$) can be strategized in real time as recourse in the second stage once the product spot price scenarios are revealed. A complete nomenclature table is presented in Table 3.1 and a detailed formulation is introduced in Section 3.3.

3.3 Model Development

As described in Section 3.2, the problem can be modeled by a framework consisting of a two-stage stochastic program and a supporting time series model (described in 3.3.2).

More specifically, first an ethanol spot price time series based on Schwartz et al. [55] is created to provide long-term ethanol spot price simulations and forecast. Second, the fixed rates of four swap contracts are calculated from the spot price forecast. Subsequently, spot price simulations are input to the two-stage stochastic program as the source of uncertainty. Finally, the two-stage stochastic program is solved to provide hedging, production, selling and storage decisions. The above framework is illustrated in the following algorithm:

Algorithm 1: Solution Framework

- 1: Estimate the Schwartz-Smith two-factor model with Iowa State ethanol weekly spot price data from 2006-2014.
 - 2: Simulate 1000 one-year ahead spot price scenarios ($spot_{i,j}$) and estimate one-year ahead spot price forecast (\bar{S}_i) from the model trained in 1.
 - 3: Input \bar{S}_i to the fixed rate formula (Equation 3.18) to calculate specific fixed rates (\bar{C}_q) corresponding to quarterly swap contracts.
 - 4: Input $spot_{i,j}$ from 2, and \bar{C}_q from 3 to the two-stage stochastic program.
 - 5: Solve the optimization model with the probability-weighted scenarios to determine the following decision variables:
 - First stage-quarterly swap contract shares (Sh_q), weekly production level ($prod_i$).
 - Second stage-weekly spot market sales ($Sa_{i,j}$), weekly storage level ($St_{i,j}$).
-

3.3.1 A two-stage stochastic program

The two-stage stochastic program aims to maximize the total expected profit and is formulated as a mixed integer linear program (MILP). In the first stage, key decision variables are production levels $prod_i$ (continuous) and shares of swap contracts Sh_q (integer). In the second stage, continuous recourse variables are weekly spot market sales $Sa_{i,j}$ and storage level $St_{i,j}$.

To facilitate description of the model, nomenclature is delineated in Table 3.1.

Nomenclature	
Sets	
i	week
j	scenario
q	quarter
Parameters	
T	total weekly operating hours
S	total number of scenarios
Q	conversion factor
FOC	fixed operating cost
FCC	annualized fixed capital
$spot_{i,j}$	simulated ethanol spot prices
$Icap$	inventory capacity
$Pcap$	production capacity
\bar{C}_q	fixed rate of ethanol swap
k_1	unit carbon tax for region 1
k_2	unit carbon tax for region 2
b	threshold hourly emission level between two regions
Cf_1	coefficients for greenhouse gas emission level
Cf_2	coefficients for variable operating cost
I	unit inventory cost
Variables	
<i>First stage variables</i>	
$prod_i$	hourly production level of week i
GHG_i	Green house gas emission rate
CT_i	carbon tax
H_q	weekly hedging level of quarter q
Sh_q	weekly contract shares of quarter q
VOC_i	variable operating cost
$Pr_{1,q}$	first stage profit
<i>Second stage variables</i>	
$Sa_{i,j}$	weekly spot market sales for scenario j
$St_{i,j}$	weekly storage level for scenario j
$Pr_{2,i,j}$	second stage profit
$cost_i$	total cost
TP_j	total profit for each scenario

Table 3.1: Nomenclature

The two-stage stochastic program is formulated as follows, where the process is not modeled in detail here. Instead, the relation between greenhouse gas emission and product (Cf_1), as well as the relation between variable operating

cost and product (Cf_2), are extracted from the process model described in Cheng and Anderson [11]. This relieves the computation complexity.

The objective is to maximize the total expected profit:

$$\max \sum_j \pi_j TP_j \quad (3.1)$$

where π_j is the probability of spot price scenario j , and TP_j is the total profit in each spot price scenario.

subject to the following constraints:

$$\begin{aligned} prod_i \times T + St_{i-1,j} &= Sa_{i,j} + H_q + St_{i,j} \\ \forall i \in 1, \dots, N \quad \forall j \in 1, \dots, S \end{aligned} \quad (3.2)$$

$$H_q = Sh_q \times Q \quad (3.3)$$

where $St_{0,j}$ is defined as zero as storage is assumed to be empty at the start of the planning horizon, and (3.2) refers to the weekly production level ($prod_i$), storage ($St_{i,j}$), spot market sale ($Sa_{i,j}$), and hedging (H_q) balance. The relation between the swap contract shares (Sh_q) and the underlying hedging amount (H_q) is given in (3.3), where there are Q tons ethanol per share of swap contract. The quarter index q is defined as: $q = \frac{i_q}{13}$ for all weeks $i_q - 12 \leq i \leq i_q$, where $i_q \in \{13, 26, 39, 52\}$. In other words, the weeks of a year are grouped into four quarters with Week 13, 26, 39, and 52 representing the end of each quarter.

The model assumes limited storage and production capacity as detailed below, where $Icap$ and $Pcap$ are the upper bound of the inventory and production level respectively. The last capacity constraint regulates the quarterly hedging

quantity should not exceed the quarterly production commitment.

$$St_{i,j} \leq Icap \quad (3.4)$$

$$prod_i \leq Pcap \quad (3.5)$$

$$H_q \leq \sum_{i=1}^{q_t} prod_i \quad (3.6)$$

A piecewise linear carbon tax is implemented in (3.7), (3.8) in accordance with Benjaafar et al. [4] and maintains the linearity of the program.

$$CT_i \geq k_1 GHG_i \quad (3.7)$$

$$CT_i \geq k_2 GHG_i + b \quad (3.8)$$

where k_1 and k_2 ($k_1 \leq k_2$) corresponds to the unit carbon tax rate for distinct emission regions while b is the intercept which keeps the continuity of the piecewise linear function.

The relation between Greenhouse gas emission level in each week (GHG_i) and production level is approximated as:

$$GHG_i = Cf_1 \cdot prod_i \quad (3.9)$$

where Cf_1 is the correlation factor between greenhouse gas emission level and production rate.

Finally, cost and profit related constraints are as follows:

$$cost_i = T \cdot CT_i + VOC_i \quad (3.10)$$

$$VOC_i = Cf_2 \cdot prod_i \quad (3.11)$$

$$Pr_{1_q} = \bar{C}_q \cdot H_q \quad (3.12)$$

$$Pr_{2_{i,j}} = spot_{i,j} \cdot Sa_{i,j} - I \cdot St_{i,j} \quad (3.13)$$

$$TP_j = \sum_{q=1}^4 Pr_{1_q} - \sum_{i=1}^{52} cost_i + \sum_{i=1}^{52} Pr_{2_{i,j}} \quad (3.14)$$

where cost in each week ($cost_i$) is comprised of carbon tax (CT_i) and variable operating cost (VOC_i), and variable operating cost is proportional to the production level. Furthermore, the first-stage ancillary profit (Pr_{1_q}) contains the revenue from selling the product by swap contract and the second-stage ancillary profit ($Pr_{2_{i,j}}$) contains spot market revenue net the storage cost. Finally, the total profit in each scenario, TP_j , is defined as the annual sum of the first-stage profit, the second-stage profit minus the cost.

The other primary element of this model framework is the stochastic process of ethanol spot price, described in Section 3.3.2.

3.3.2 A long-term time series model for ethanol spot price

Early studies in commodity price modeling typically assumed the commodity price followed Geometric Brownian Motion (GBM) since this distribution is used to model stock price in the famous Black-Scholes option pricing formula. Later, research showed a mean-reverting price model would be more appropriate for commodity price series due to the underlying supply-demand equilibrium [24]. Schwartz et al. [55] discovered that although the commodity price appeared to be mean-reverting, the equilibrium price remained uncertain. As a response, a two-factor model was developed and has been adopted ever since for long-term commodity price modeling [8, 22].

The two-factor model represents the spot price at time t , denoted as S_t as a function of two stochastic factors:

$$\ln(S_t) = \chi_t + \xi_t \quad (3.15)$$

where χ_t depicts the short term deviation and follows a mean reverting process:

$$d\chi_t = -\kappa\chi_t dt + \sigma_\chi dz_\chi \quad (3.16)$$

the equilibrium level ξ_t is modeled as a Brownian motion process:

$$d\xi_t = \mu_\xi dt + \sigma_\xi dz_\xi \quad (3.17)$$

The terms dz_χ and dz_ξ are correlated increments of a standard Brownian motion process, such that $dz_\chi dz_\xi = \rho_{\chi\xi} dt$. In order to simulate the spot price process, it is essential to have an accurate estimation of the process parameters, namely $\kappa, \sigma_\chi, \mu_\xi, \sigma_\xi$, and $\rho_{\chi\xi}$. However, these parameters are associated with two “hidden processes”, χ_t , and ξ_t , whose values are not directly observable. Therefore, the Kalman filter is used to estimate their values [26]. For detailed steps of applying Kalman filter in a two-factor model parameter estimation, spot price forecast and simulation, interested readers are referred to [22]. Once the time series for the ethanol spot prices is established, the fixed rates of the four ethanol swap contracts can be determined from the spot price forecast. This process is described in Section 3.3.3.

3.3.3 A simple pricing formula for ethanol swap contracts

A commodity swap contract is an agreement between two parties to exchange a series of cash payments generated by the underlying assets over a specified period for the purpose of securing the selling price of the underlying asset [27]. No physical commodity is transferred between the two parties. Specifically in energy swap contracts, the energy producer is willing to pay a floating rate to the counter-party in exchange for a fixed rate so, in effect, the underlying energy

product is sold at a fixed price (see Figure 3.1). While the floating rate is mainly based on the spot price of the commodity, the fixed rate is determined in the contract.

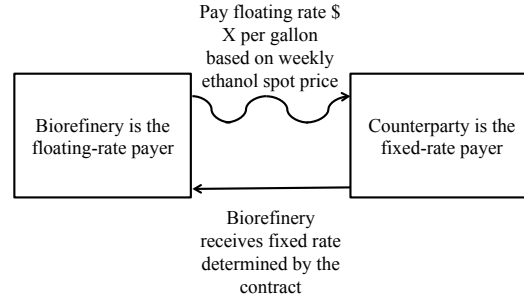


Figure 3.1: Bioethanol hedging using swap contracts

As stated in Section 3.2, four quarterly-matured swap contracts are considered, each of which has weekly payments within the quarter. The initiation and maturity sequence of the four swap contracts is illustrated in Figure 3.2. Under the no-arbitrage pricing scheme, the fixed rate of an ethanol swap contract, \bar{C} is priced by the following formula [19]:

$$\sum_{t=T_1}^{T_N} \frac{\bar{C}}{(1+r_t)^t} = \sum_{t=T_1}^{T_N} \frac{C_t}{(1+r_t)^t} \quad (3.18)$$

where C_t is the time-varying ethanol spot price forecast at time t , r_t is the risk-free rate at time t , T_1 and T_N are the initial date and the maturity date of the swap contracts respectively.

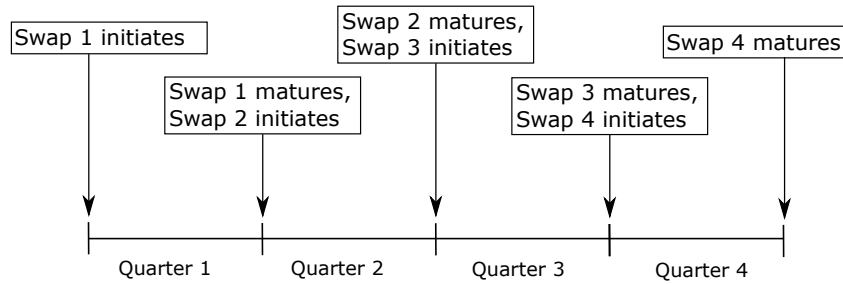


Figure 3.2: The sequence of the four swap contracts used in the model

3.4 Results

In this section, the parameterization of the Schwartz-Smith two-factor time series model is discussed first. The second stage ethanol spot price process is then represented with a sample of (1000) price trajectories from the Schwartz-Smith model. The stochastic program determines a portfolio of long-term strategies to maximize the total expected profit and has 161,225 variables and 161,274 constraints. A risk neutral case is first considered, as formulated by constraints Equation 3.2-3.14. A risk averse case is considered next, in which operator is able to define their own risk level by incorporating additional risk constraints (defined in Section 3.4.4). And finally, a discussion of sensitivity is performed, in which the impact of alternative spot price trajectories and storage capacities have been explored (Section 3.4.5). All the optimization models are solved with CPLEX 12.5.0.1.

3.4.1 Results for Schwartz-Smith (SS) two-factor models

The SS two-factor ethanol spot price model was built on training data corresponding to weekly New York Ethanol (Platts) Futures one month, three months, five months, nine months, and eleven months to maturity, as well as the Iowa state spot prices from November 2006 to September 2014. All historical spot price data was obtained from [5]. The parameter estimates for the ethanol spot price SS two-factor model are summarized in Table 3.2.

Parameter	κ	σ_χ	μ_ξ	σ_ξ	$\rho_{\chi\xi}$	s_1	s_2	s_3	s_4	s_5
Value	0.32	0.76	-0.056	0.64	-0.92	0.0015	0	0	0	0.088

Table 3.2: Parameter values for the SS two-factor model.

A table (Table 3.3) comparing the goodness of fit of the two-factor model and Geometric Brownian Motion in terms of Akaike information criterion (AIC) and Bayesian information criterion (BIC) is also presented. Since the two-factor

Model	AIC	BIC
two-factor model	15.32	56.28
GBM	16.07	57.76

Table 3.3: Model selection criteria for two reference models

model demonstrates lower AIC and BIC values than Geometric Brownian Motion, it is safe to assume the two-factor model outperforms GBM in modeling the ethanol spot time series.

The spot price simulations, which represent possible annual price trajectories in the future, are shown in Figures 3.3 and 3.4. These figures illustrate year 2014 spot price and one-year ahead conditional expectation forecast with the associated range of uncertainty. Rather than reflecting a specific price pattern in the future one year, the forecast price demonstrates a scenario mean trend, which is the requirement to determine the fair price of the swap contracts. The decreasing trend of the forecast price observed in Figure 3.4 corresponds to the recent ethanol spot price pattern.

In the following sections, the SS two-factor model is used as input to represent ethanol price uncertainty.

3.4.2 Production schedule and hedging decisions

In this section, the results of the stochastic optimization model are presented. For this purpose, the key parameter values for the case-study are listed in Table

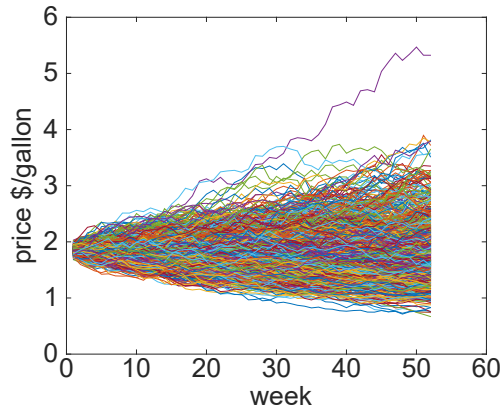


Figure 3.3: A Sample set of weekly ethanol spot price scenarios

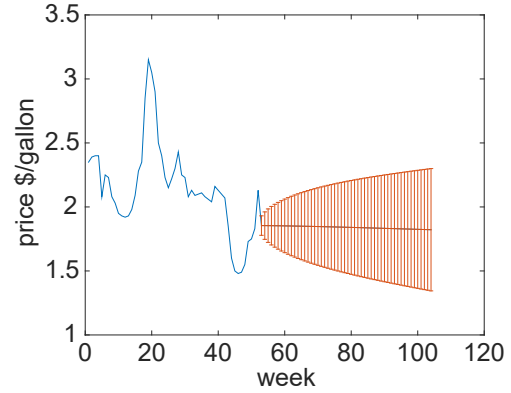


Figure 3.4: weekly spot price and one-year ahead price forecast w bars.

3.4.

The optimization model is solved using the price scenarios and fixed rates determined in the previous sections. The key decision variables in the first-stage are weekly production levels and quarterly hedging levels. Figure 3.5 shows that the weekly production level follows a decreasing trend and is influenced by both scenario mean spot prices and second region unit carbon tax rates. As the scenario mean spot prices decrease over time, the optimal production level experiences a decline from full capacity, approximately 20 *ton/h*, to partial capacity, approximately 10 *ton/h*. The second region carbon tax rate (k_2 in the model) also plays an important role. From the lower bound, 620 \$/ton *GHG* to the upper bound, 640 \$/ton *GHG*, a higher second region unit carbon tax always leads to a decrease of the production level. In the extreme case of carbon tax 640 \$/ton *GHG*, the production level stays at approximately half capacity (10 *ton/h*) throughout the planning period. This result is counter-intuitive, since typically a positive marginal profit leads to maximum production, though in this case carbon tax can become prohibitive. The sporadic production decrease

Table 3.4: Case-Study Parameters for two-stage stochastic program

Parameter	Value
Scenario probability (π_j)	0.001 ¹
Conversion factor (Q)	125 ton/share
Storage capacity (I_{cap})	14816 ton
Production capacity (P_{cap})	20 ton/hour
Unit carbon tax for region 1 (k_1)	50 ton/hour
Unit carbon tax for region 2 (k_2)	varies
Threshold hourly emission level (b)	varies with k_2
GHG coefficient (Cf_1)	0.98
Variable operating cost coefficient (Cf_2)	451.8 \$/ton
1 st fixed rate (\bar{C}_1)	1.85 \$/gallon
2 nd quarter fixed rate (\bar{C}_2)	1.84 \$/gallon
3 rd quarter fixed rate (\bar{C}_3)	1.83 \$/gallon
4 th quarter fixed rate (\bar{C}_4)	1.82 \$/gallon
Storage cost (I)	10 \$/ton

¹ Since every scenario is generated with equal weights, the probability for each scenario is $\frac{1}{N}$, where N is 1000 here.

at intermediate-high carbon tax cases, i.e. k_2 equals to 632 – 636 \$/ton GHG, shows that the profit margins are small enough that the producers' optimal production strategy is influenced by storage capability. In this case, producing at a higher capacity requires higher marginal profit to overcome carbon tax expenses. The operator can achieve this higher profit through inter-temporal arbitrage with storage. When storage reaches full capacity, the production level decreases. As stored product is sold, and storage capacity once again becomes available, the production level returns to a higher value to rebuild inventory in anticipation of higher future prices. At lower carbon tax rates, it is profitable

to produce ethanol at full capacity, regardless of the available storage capacity. It is worth noting that the choice of the second region unit carbon tax rate, ranging from 620 $\$/\text{ton GHG}$ to 640 $\$/\text{ton GHG}$, is higher than any current practice in existence. However, this choice is used as an indication of the impact of stringent carbon tax policy on the optimal operation decisions.

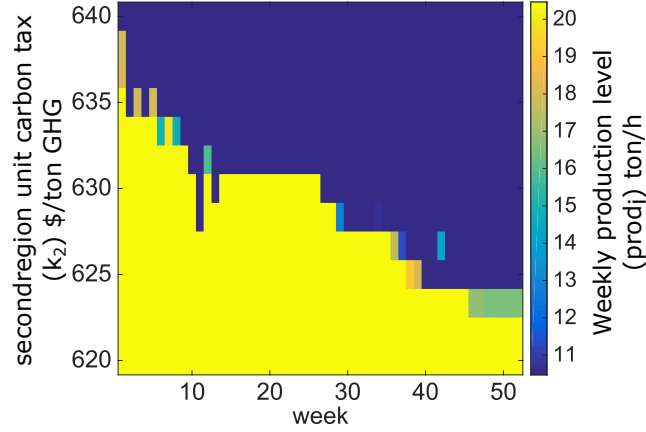


Figure 3.5: Weekly production levels corresponding to second region unit carbon taxes (k_2), with decreasing spot price trend, shows that increasing carbon tax leads to declining production.

In the first stage, the ratio of ethanol to be hedged via swap contracts are also determined. In this case, the second region unit carbon rate is fixed to be 630 $\$/\text{ton GHG}$ and weekly scenario mean spot price is drawn as a proxy to represent the forecasted price trend. Figure 3.6 displays the optimal hedging level (blue line), the production level (red line), the spot price forecast (black line) and is compared with Figure 3.7, where the same set of decision variables are illustrated for a synthetic case with no storage.

Comparison of Figure 3.6 and 3.7 shows the influence of inventory on production and sales strategy. Specifically, the optimal hedging level is not only impacted by spot price forecast, but also by storage capacity. Specifically, in the absence of storage, production decisions are well behaved and consistent with

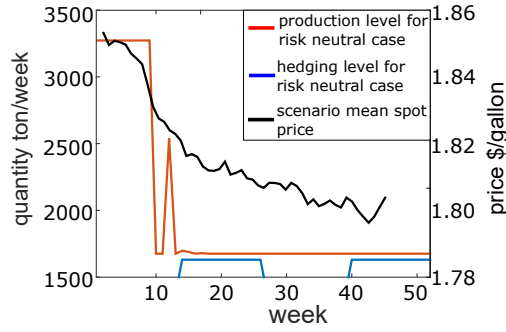


Figure 3.6: Production and hedging level with storage

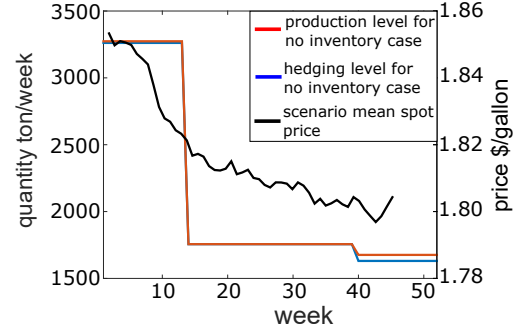


Figure 3.7: Production and hedging level with no storage capacity

the price trajectory; what is produced is hedged and production declines with lower product prices. Conversely, with the ability to store product, although the production level declines in general, a spike in production occurs when storage becomes available (approximately week 12 in Figure 3.6), to allow for potentially favorable future prices. This shows that while financial risk can be managed with hedging contracts, the capability to store product provides additional benefits to the producer.

3.4.3 Storage and selling decisions

In the second stage, recourse decisions, such as weekly sales on spot market and storage level, are made based on updated spot price information. Among the total one thousand spot price realizations, decisions for three scenarios, which represent a high spot price, a medium spot price and a low spot price are plotted in Figure 3.8.

Regardless of the spot price realizations, sales on the spot market declines dramatically in the later quarters, which tallies with the full hedging strategy

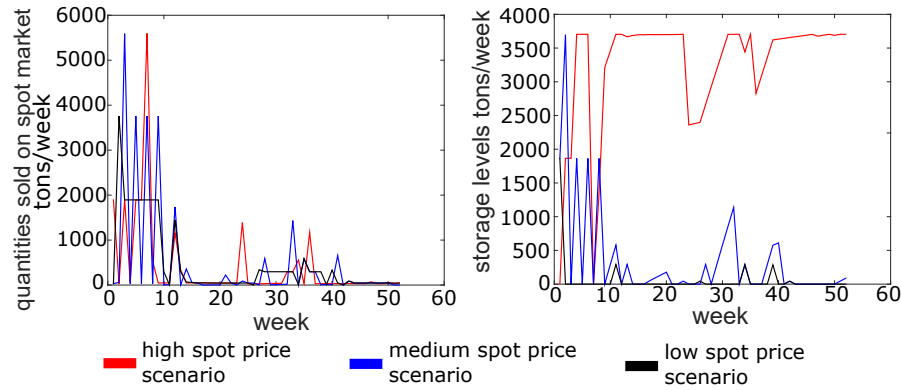


Figure 3.8: Sales and storage behavior for high, medium, and low spot price trends: ethanol spot market sales (left panel) and storage level (right panel)

decided in the first stage. However, the relation between the spot price and selling on the spot market is indistinctive due to the fact that larger part of the product is hedged with a fixed rate rather than exposed to the spot price, so ethanol sales are less sensitivity to spot price fluctuations in the second stage.

The storage level, on the other hand, exhibits distinct behavior for different spot price scenarios. In the high spot price scenario, the storage level features on an escalation trend, which allows the decision maker to maximize their profit by postponing the sales on the spot market. In both medium and low spot price scenarios, an oscillation and reduction pattern persists due to the decision maker's dichotomous choice of either "hedging for now" or "waiting, and seeking a higher price in the future". It is obvious that the lower spot price scenario always favors the choice of hedging over storing.

3.4.4 Risk management with cVaR constraints

In addition to hedging with swap contracts, the model can be further tuned to include the operator's preference for more stable revenues. In this section, these risk preference levels are considered by adding the following cVaR constraints [31].

$$z_j = [TP_j - VaR]^- \quad (3.19)$$

$$cVaR = VaR + \frac{1}{1 - \alpha} \sum_j \pi_j z_j \quad (3.20)$$

$$cVaR \geq K \quad (3.21)$$

where z_j is a nonpositive auxiliary variable, VaR and $cVaR$ are value-at-risk, and conditional value-at-risk at probability level α , and K is a user-defined risk level. In the practical setting, the model with cVaR constraints informs the operator of the precise shares of swap contracts in hedging, thus leading to customized risk management.

Table 3.5 compares the profit distribution for the risk neutral case (without risk management) to two risk averse cases with different risk-level constraints. And the tradeoff between a reduced total expected profit and increased profit certainty is shown for different cases.

Example	E[profit]/million \$	normalized std
risk neutral case	6.50	0.212
cVaR $\geq 6.4 \times 10^6$	6.49	0.123
cVaR $\geq 6.43 \times 10^6$	6.46	0.0466

Table 3.5: Expected profit and normalized standard deviation for decreasing risk levels

An increased cVaR level corresponds to a higher risk aversion level and less sale on spot market, thus leading to higher certainty in profit distribution and less expected total profit. In the extreme case of $cVaR \geq 6.43 \times 10^6$, the

cVaR achieves maximal achievable value, above which the optimization program becomes infeasible. The resulting profit becomes significantly lower but more deterministic. This implies the model not only selects the optimal number of contract under various risk aversion levels, but also informs the maximum achievable risk aversion level given the spot price and the availability of swap contracts.

Figure 3.9 provides the optimal hedging strategy for producers at different risk levels. The number of swap contracts at higher risk aversion levels is consistently more than the lower risk aversion levels. At the extreme, full hedging throughout the entire production period leads to a constant selling price.

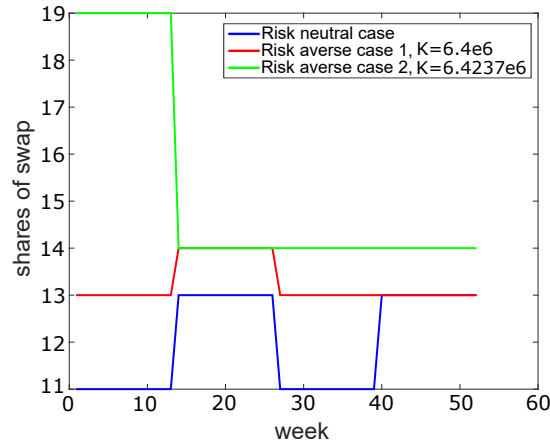


Figure 3.9: Shares of swap entered for decreasing risk levels

3.4.5 Sensitivity Analysis

The results presented thus far have been based on specific spot price forecast patterns and storage capacity. It is worthwhile to consider alternative spot price patterns and storage capacities to test the sensitivity of the optimal strategy to

these factors. Throughout this section, the risk averse case is used as with cVaR lower bound (K) setting to 0.

Spot price patterns

In order to investigate the impact of spot price patterns on production decisions, three other sets of spot price scenarios are simulated. As the price scenario of the risk averse case is generated from a two-factor model, it is necessary to use the same time series model to generate other spot price patterns. Therefore, different lengths of the original dataset are applied as the training datasets. The characteristics of the spot price patterns and the specific periods are listed in Table 3.6. These patterns are input to the two-stage stochastic program to determine the resultant strategies for each case. Figure 3.10 represents the optimal production levels for each of the alternative patterns. Here the red line is the scenario mean spot price forecast, which represents different spot price forecast patterns. Results show that production level encounters a switch once the spot price reaches a threshold. For example, in the case of rapid increase, gradual decrease, and rapid decrease pattern, the price threshold that triggers the production switching occurs around 1.8 \$/gallon. In the gradual increase case, the production remains at full capacity throughout the planning period because the minimum forecast price is well above 1.8 \$/gallon.

Spot price patterns	Range of weeks
Gradual increase	1-200
Rapid increase	1-250
Gradual decrease (risk averse case)	1-426
Rapid decrease	1-400

Table 3.6: Alternative spot price patterns, generated from historical data (weeks indicated)

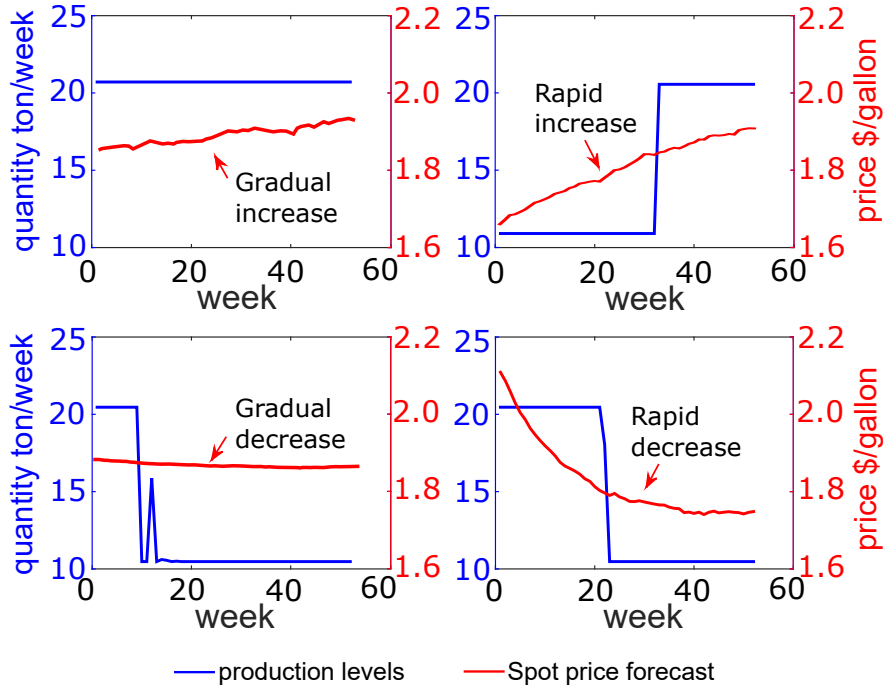


Figure 3.10: Production levels for alternative spot price trends

As previously discussed, the storage capacity influences the hedging level within the planning horizon. Therefore, the next section examines the effect of a range of storage capacities on the hedging levels and profit distributions,

Storage capacity

Four capacity values, i.e. 25%, 50%, 200%, and 400% of risk averse case capacity are explicitly selected to compare with the risk averse case. The risk level is set to be $cVaR \geq 6.4 \times 10^6$ for all storage capacities. The expected total profit and the normalized standard deviation for these cases are compared in Table 3.7. Shares of contract entered are plotted in Figure 3.11.

At the same risk level, cases with higher storage capacity seek to maximize the expected profit by using fewer swap contracts in Q1 when the spot price is

Examples	E[profit]/million \$	normalized std
25% <i>Icap</i>	6.44	0.0557
50% <i>Icap</i>	6.46	0.0802
risk averse case	6.49	0.123
200% <i>Icap</i>	6.55	0.189
400% <i>Icap</i>	6.63	0.291

Table 3.7: Expected profit and normalized standard deviation for cases with different storage capacity, showing that higher storage capacity leads to higher expectation and standard deviation of profit, at the same risk level.

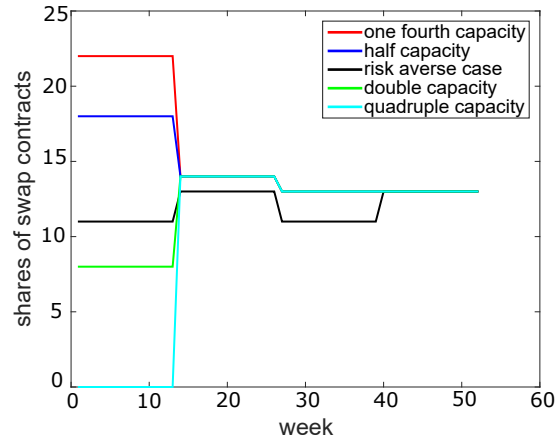


Figure 3.11: Hedging level for risk averse case and different storage capacities, note higher storage capacity leads to more storage in Q1, thus decreasing the shares of swap contracts used

relatively high. Higher storage capacity provides the flexibility of storing more and selling at higher spot price periods. When the spot price declines to unfavorable region, as is seen in Q2, Q3 and Q4, the product is fully hedged across all the cases, leading to both an identical number of swap contracts throughout different storage capacity and an equal value of risk aversion level. In conclusion, cases with higher storage capacity increase total profit by exploiting the storage capacity and spot sales in Q1.

3.5 Conclusion

This study has presented a framework to determine the optimal production, hedging, selling and storage decision for a dilute-acid pretreatment based lignocellulosic biorefinery. A two-stage stochastic program is formulated in light of the decision sequence, while the underlying spot price is characterized by a Schwartz-Smith two factor model. In the first stage, weekly production is jointly determined by carbon tax rate and scenario mean spot price trend. Under the parameter setting presented, it is observed that the production level switches from full capacity to half capacity once the scenario mean spot price falls below 1.8\$/gallon. Moreover, customized risk management decisions can be obtained by adjusting the conditional value-at-risk constraint (Equation 3.21) in the model. The corresponding optimization results represent a tradeoff between the shares of swap contract to enter and the inventory level. In other words, a dynamic balance between “hedge for now” and “store, and seek a higher price in the future” is achieved.

In the second stage, strategies for spot market sales, and storage levels are scenario-specific, and are recourse to facilitate further increase of the total profit. In the three representative spot price scenarios, it has been shown that while sales on the spot market are largely governed by hedging level, the storage level positively correlates to spot price patterns.

Finally, it has been demonstrated that higher storage capacity also boosts the facility’s profit. At the same risk preference level, a higher storage capacity leads to increasing storage level and fewer shares of swap contracts to enter. In other words, the storage capability enables the possibility of postponing the sale of

the product to high price periods.

CHAPTER 4

VALIDATION OF THE MODEL FRAMEWORK IN A FIRST GENERATION BIOREFINERY

Since the aim of this chapter is to validate the optimal production and hedging model framework developed in the previous chapter, the model framework is applied to a first generation biorefinery to determine the weekly production level and swap hedging portfolios over a year's planning horizon with the objective of maximizing the process profit. A back test program is then created to compare the realized profit obtained from applying the optimal decisions and the negotiated profit derived from using the current practice. This comparison in turn validates the effectiveness of the proposed model framework.

4.1 Introduction

After a decade of hectic searching for economical processes converting corn to bioethanol, the nationwide "biofuel rush" is now waning as people are increasingly cautious about process profitability. The crash of KiOR [17] as well as the bankruptcy of VeraSun Energy [41] are among the most prominent indications of the ongoing retrenchment in the biofuel sector. Moreover, Renewable Fuel Standard (RFS2, [16]), which regulates the total renewable fuel requirement increasing to 36 billion gallons a year in 2022 by EPA, has been under criticism due to its aggressiveness. One of the looming problems hampering the commercial viability of bioethanol is the thin profit margin in a volatile energy market. Therefore, how to maintain an appreciable level of profit during adverse market conditions is a pressing problem awaiting researchers' answer. Interviews

with the industry practitioners have shown that the operators tend to be extremely risk averse. Hence, they prefer locking their corn purchase and ethanol sale prices by entering into long-term fixed rate contracts. Consequently, a fixed profit or loss is obtained depending on the negotiated fixed rates. Although this industry practice completely eliminates the profit uncertainty and simplifies the decision-making process, potential profit may be lost. Therefore, a more sophisticated operating and risk management decision framework is imperative to enhance the profit margin.

The key contributions of this chapter are:

- Although various models are assumed for the ethanol spot prices in the previous chapters, while these models are valid for ethanol spot prices in different time horizons, they fail to depict the correlation between corn and ethanol spot prices (formally shown in Section 4.3). Since a corn biorefinery encounters price uncertainties from both corn and ethanol side, an appropriate model should consider the correlation between these two price processes. Specifically, a bivariate vector error correction model (VECM) is applied in the current paper to simulate the corn and ethanol spot prices.
- Compared with the previous studies invoking a real option approach to determine the projects' profitability and entry/exit threshold margin [54, 53, 30, 38, 39, 34], this study extends the richness and flexibility of operation and hedging decisions. To be more specific, unlike the aforementioned works that address binary planning decision of switching on or off, this study also investigates the weekly optimal production level while adding hedging decisions as an extra layer of profit protection.

- Since the unique emphasis of this study is to provide the industry practitioner with the insight into using financial derivatives to exploit the potential profit, the production and hedging strategies determined from the optimization model are compared with the current industry practice using the real spot price data from 2010 to 2016. Although previous works such as Cheng and Anderson [11] and Cheng et al. [12] have explored both the short term and long term optimal decisions for a biorefinery, their target is a demonstration scale lignocellulosic biorefinery and the decisions are not tested on real world problems.

The remainder of the chapter is organized as follows. Section 4.2 describes the problem in detail. In Section 4.3, the optimization model is formulated and time series model described. Results are provided and discussed in Section 4.4. Finally, conclusions are delineated in Section 4.5.

4.2 Problem Statement and Assumptions

Given a corn biorefinery facility exposed to two major external uncertainties: corn and ethanol spot prices, the goal is to determine the long-term corn supply, ethanol production and hedging strategies to maximize the facility's total profit and control the financial risk. The target biorefinery drawn from Mcaloon et al. [40] has the process flow diagram in Figure 4.1. It is further assumed that there exist five swap contracts for both corn and ethanol that mature in March (Week 12), May (Week 21), July (Week 30), September (Week 39) and December (Week 53) respectively. The choice of five swap contracts matches the trading calendar of corn derivatives that are active on Chicago Board of Trade (CBOT).

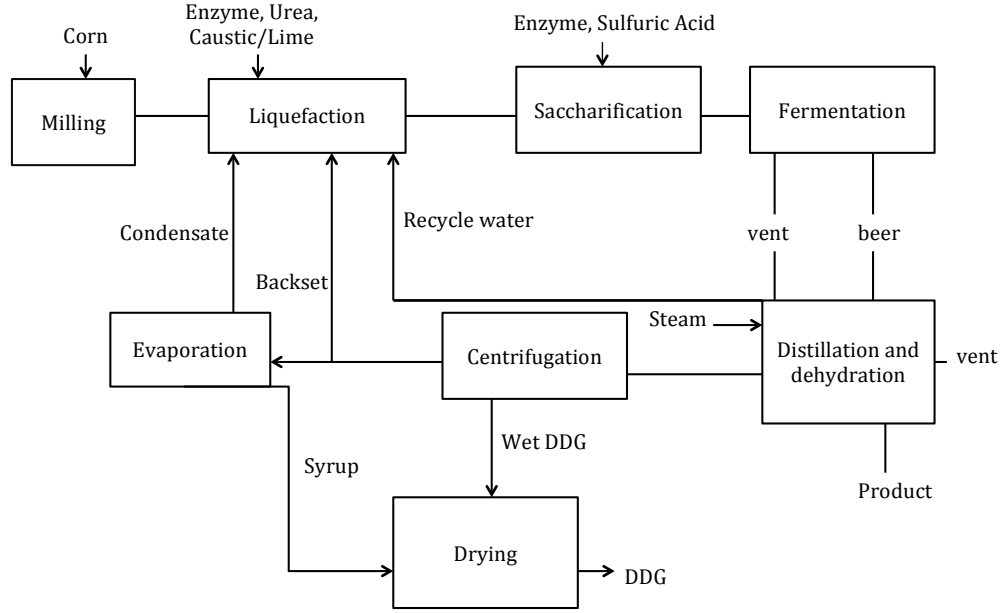


Figure 4.1: Process flow for corn biorefinery

This choice of swap contracts also maintains the long term hedging framework while ensuring the strategy flexibility. Although it is possible to use swap contracts with longer tenor, such as one-year, this will result in a suboptimal profit level as the operator loses the flexibility to adjust the hedging decisions.

Such a strategic planning problem can be further decomposed into two sets of decisions, first the weekly corn supply, ethanol production schedule, and the swap contract hedging level over a year, and second, the weekly spot market corn purchase and ethanol sale decisions. The choice of hedging and production plan in an annual time frame corresponds with the goal of long-term planning, whereas weekly purchase and sale decisions ensures the flexibility to adjust to different price scenarios.

In the world of stochastic programming, such a problem can be formulated as a two-stage stochastic program. Under the commonly acknowledged no-

arbitrage financial assumption, long-term contractual hedging (Hc_q and He_q), corn supply (fs_i) and production decisions ($prod_i$) need to be determined in the first stage before observing any spot price information ($Pc_{i,j}$ and $Pe_{i,j}$), whereas quick responses, such as ethanol spot sale ($Se_{i,j}$) and corn spot purchase ($Sc_{i,j}$) can be strategized in real time as recourse in the second stage once the product spot price scenarios are revealed. A complete nomenclature table is presented in Table 4.1 and a detailed formulation is introduced in Section 4.3.

4.3 Model Development

As described in Section 4.2, the problem can be modeled by a framework consisting of a two-stage stochastic program, a supporting time series model (described in 4.3.2) and a back testing model (described in 4.3.4).

More specifically, for each year between 2010 and 2016, first a bivariate vector error correction model (VECM) is created to provide long-term corn and ethanol spot price simulations and forecast of that year [56]. Second, the fixed legs (the straight line in Figure 4.2) of the five swap contracts are calculated from the spot price forecast. Subsequently, spot price simulations are input to the two-stage stochastic program as the source of uncertainty. Furthermore, the two-stage stochastic program is solved to provide hedging, supply, production, spot purchase and spot sale decisions. Finally, the optimal decisions are extracted and are input to the back testing model to compute the realized profit of that year. This profit is then compared with the negotiated profit earned from using the current industry practice (explained further in 4.3.4). The above framework is illustrated in the following algorithm:

Algorithm 2: Solution Framework

- 1: **for** $yr = 2010$ to 2016 **do**
 - 2: Estimate the parameters of VECM using corn and ethanol spot price data from 2008 up till $yr - 1$.
 - 3: Simulate 1000 one-year ahead spot price scenarios ($P_{c_{i,j}}$ and $P_{e_{i,j}}$) and estimate one-year ahead spot price forecast ($\overline{P_{c_i}}$ and $\overline{P_{e_i}}$) from the model trained in 2.
 - 4: Input $\overline{P_{c_i}}$ and $\overline{P_{e_i}}$ to the fixed leg formula (Equation 4.16) to calculate specific fixed legs ($\overline{C_{c_q}}$ and $\overline{C_{e_q}}$) corresponding to the corn and ethanol swap contracts at different periods.
 - 5: Input $P_{c_{i,j}}$ and $P_{e_{i,j}}$ from 3, and $\overline{C_{c_q}}$ and $\overline{C_{e_q}}$ from 4 to the two-stage stochastic program.
 - 6: Solve the optimization model with the probability-weighted scenarios to determine the following decision variables:
 - First stage-swap contract shares for both corn and ethanol in each period (N_{c_q} and N_{e_q}), weekly corn supply (f_{s_i}), and ethanol production level ($prod_i$).
 - Second stage-weekly corn spot purchase $S_{c_{i,j}}$ and ethanol spot sale $S_{e_{i,j}}$.
 - 7: Input the decision variables from 6 and the realized ethanol and corn spot prices (\mathcal{P}_{c_i} and \mathcal{P}_{e_i}) of Year yr to the back testing model to calculate the realized profit (\mathcal{P}_r).
 - 8: Use spot price scenario mean ($\overline{P_{c_{i,j}}}$ and $\overline{P_{e_{i,j}}}$) as the negotiated fixed rate to calculate the negotiated profit from current industry practice (\overline{Pr}) (further elaborated in Section 4.3.4).
 - 9: Compare the realized profit (\mathcal{P}_r) and the negotiated profit (\overline{Pr}).
 - 10: **end for**
-

4.3.1 A two-stage stochastic program

The two-stage stochastic program aims to maximize the total expected profit and is formulated as a mixed integer linear program (MILP). In the first stage, key decision variables are corn supply fs_i , ethanol production $prod_i$ (continuous) and shares of swap contracts $N_{c_q} N_{e_q}$ (integer). In the second stage, continuous recourse variables are weekly corn spot purchase $Sc_{i,j}$ and ethanol spot sale $Se_{i,j}$.

To facilitate description of the model, nomenclature is delineated in Table 4.1.

Nomenclature	
Indices	
i	week
j	scenario
q	swap contracts sequence
Parameters	
π_j	probability of scenario j (identical for each scenario in this study)
T	total weekly operating hours
S	total number of scenarios
Q_c	conversion factor from the physical quantity to shares of corn swap contracts
Q_e	conversion factor from the physical quantity to shares of ethanol swap contracts
$Pc_{i,j}$	simulated corn spot prices
$Pe_{i,j}$	simulated ethanol spot prices
$Pcap$	production capacity
$\overline{Cc_q}$	fixed leg of the q-th corn swap contract
$\overline{Ce_q}$	fixed leg of the q-th ethanol swap contract
Cf_1	coefficients for ethanol production level
Cf_2	coefficients for operating cost
K	user-defined risk preference level
α	percentile of the profit distribution

Table 4.1: Nomenclature

Nomenclature Cont'd

Variables

First stage

fs_i	hourly corn supply level of week i
$prod_i$	hourly ethanol production level of week i
Hc_q	weekly hedging level of using the q -th corn swap contract
He_q	weekly hedging level of using the q -th ethanol swap contract
Nc_q	weekly contract shares of using the q -th corn swap contract
Ne_q	weekly contract shares of using the q -th ethanol swap contract
OC	operating cost
Pr_{1_q}	first stage profit

Second stage

$Sa_{i,j}$	weekly spot market sales for scenario j
$St_{i,j}$	weekly storage level for scenario j
$Pr_{2_{i,j}}$	second stage profit
TP_j	total profit for each scenario
z_j	auxiliary nonpositive variable corresponding to each scenario
VaR	value-at-risk
$cVaR$	conditional value-at-risk

The two-stage stochastic program is formulated as follows, where the detailed chemical conversion process is not modeled here. Instead, the relationship between the ethanol production and corn supply (Cf_1), as well as the relationship between the operating cost and the production (Cf_2), are extracted from the process parameter table described in Mcaloon et al. [40]. This relieves the computation complexity.

The objective is to maximize the total expected profit:

$$\max \sum_j \pi_j TP_j \quad (4.1)$$

where π_j is the probability of spot price scenario j , and TP_j is the total profit in each spot price scenario.

subject to the following constraints:

$$\begin{aligned} fs_i \times T &= Sc_{i,j} + Hc_q \\ prod_i \times T &= Se_{i,j} + He_q \end{aligned} \quad (4.2)$$

$$\forall i \in 1, \dots, N \quad \forall j \in 1, \dots, S$$

$$\begin{aligned} Hc_q &= Nc_q \times Q_c \\ He_q &= Ne_q \times Q_e \end{aligned} \quad (4.3)$$

where (4.2) refers to the balance between weekly supply, denoted fs_i (or production, $prod_i$), hedging, denoted Hc_q and He_q , and spot purchase, denoted $Sc_{i,j}$, (or spot sale, $Se_{i,j}$). The relationship between the swap contract shares (Nc_q and Ne_q) and the underlying hedging amount (Hc_q and He_q) is given in (4.3), where there are Q_c tons corn per share of corn swap contract, and Q_e tons of ethanol per share of ethanol swap contract. The swap contract sequence index q is defined as: $q = i$ for all weeks from $i_{q-1} + 1$ to i_q , where $i_q \in \{0, 11, 20, 29, 38, 53\}$ (See Figure 4.3). In other words, the weeks of a year are grouped into five periods with Week 11, 20, 29, 38 and 53 representing the end of each period.

The model assumes limited production capacity as detailed below, where $Pcap$ is the upper bound on the production level. The last capacity constraint regulates the hedging quantity, which should not exceed the supply/production commitment.

$$prod_i \leq Pcap \quad (4.4)$$

$$Hc_q \leq \sum_{i=1}^{qT} fs_i \quad (4.5)$$

$$He_q \leq \sum_{i=1}^{qT} prod_i \quad (4.6)$$

The relationship between the weekly ethanol production ($prod_i$) and the corn supply level (fs_i) is approximated as:

$$prod_i = Cf_1 \cdot fs_i \quad (4.7)$$

where Cf_1 is the linear relationship factor between corn supply level and ethanol production rate.

The cost and profit related constraints are as follows:

$$OC_i = Cf_2 \cdot prod_i \quad (4.8)$$

$$Pr_{1_q} = \overline{Ce_q} \cdot He_q - \overline{Cc_q} \cdot Hc_q \quad (4.9)$$

$$Pr_{2_{i,j}} = Pe_{i,j} \cdot Se_{i,j} - Pc_{i,j} \cdot Sc_{i,j} \quad (4.10)$$

$$TP_j = \sum_{q=1}^5 Pr_{1_q} - \sum_{i=1}^{52} OC_i + \sum_{i=1}^{52} Pr_{2_{i,j}} \quad (4.11)$$

where the operating cost in each week (OC_i) is proportional to the production level. Furthermore, the first-stage ancillary profit (Pr_{1_q}) contains the net revenue from selling the product by swap contract and the second-stage ancillary profit ($Pr_{2_{i,j}}$) contains the net spot market sale revenue. The total profit in each scenario, TP_j , is defined as the annual sum of the first-stage profit, the second-stage profit minus the operating cost.

Finally, the model also includes the risk management constraints to meet the operator's preference for more stable revenues by adding the following cVaR constraints [31].

$$z_j = [TP_j - VaR]^- \quad (4.12)$$

$$cVaR = VaR + \frac{1}{1-\alpha} \sum_j \pi_j z_j \quad (4.13)$$

$$cVaR \geq K \quad (4.14)$$

where z_j is a nonpositive auxiliary variable, VaR and $cVaR$ are the value-at-risk, and the conditional value-at-risk at probability level α , and K is a user-defined risk preference level. In the practical setting, the model with cVaR constraints informs the operator of the precise shares of swap contracts in hedging, thus leading to customized risk management.

The other primary element of this model framework is the stochastic process of corn and ethanol spot prices, described in Section 4.3.2.

4.3.2 A bivariate time series model for corn and ethanol spot prices

Among the numerous effort to quantify the correlation between corn and ethanol spot prices, the works of Nobel laureates Clive Granger and Robert Engle [15] have become the foundation. Their works have shown with vector error correction model (VECM), both nonstationarity and cointegration can be formally characterized. Furthermore, short-term and long-term dynamics can also be fully informed. In the recent decades, the predominant methodology in the field of energy economics consist of cointegration analysis and developing different variants of the VECM [56]. As the primary focus of this study is not on the development of novel time series models, the original VECM is adopted and described below.

The VECM represents the first order difference of the joint spot price processes at time t , denoted as ΔP_t , is related to both the joint spot price at time

$t - 1$ and the earlier first order differences:

$$\Delta P_t = CP_{t-1} + \sum_{i=1}^q B_i \Delta P_{t-i} + \epsilon_t \quad (4.15)$$

where $P_t = [P_{C_t}, P_{E_t}]^T$ is the joint corn and ethanol spot price vector at time t , $\Delta P_t = P_t - P_{t-1}$, B_i and C_i are model parameters, and ϵ_t is a white noise process with mean zero and variance σ^2 . It can be observed that after collecting the terms, VECM can be converted to a corresponding vector autoregressive model of order $q+1$ (VAR($q+1$)), from which the model parameters can be easily estimated via standard routine.

4.3.3 A simple pricing formula for ethanol swap contracts

A commodity swap contract is an agreement between two parties to exchange a series of cash payments generated by the underlying assets over a specified period for the purpose of securing the selling price of the underlying asset [27]. No physical commodity is transferred between the two parties. Specifically in energy swap contracts, the energy producer is willing to pay a floating leg to the counter-party in exchange for a fixed leg so, in effect, the underlying energy product is sold at a fixed price (see Figure 4.2). While the floating leg is mainly based on the spot price of the commodity, the fixed leg is determined in the contract. Similarly, as a consumer of the corn, the biorefinery producer will pay the fixed leg in return for a floating leg to lock in the purchasing price.

As stated in Section 4.2, five swap contracts are considered for both corn and ethanol, each of which has weekly payments within its active period. The initiation and maturity sequence of the five swap contracts is illustrated in Figure 4.3. Under the no-arbitrage pricing scheme, the fixed leg of an ethanol swap

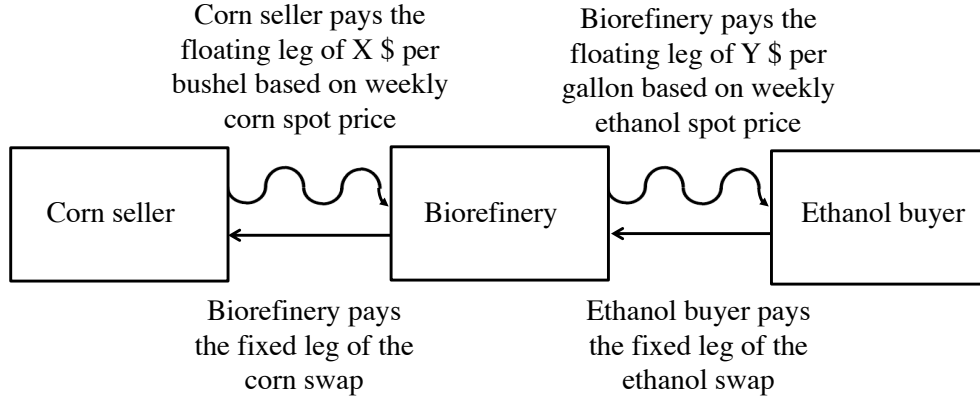


Figure 4.2: Bioethanol hedging using swap contracts

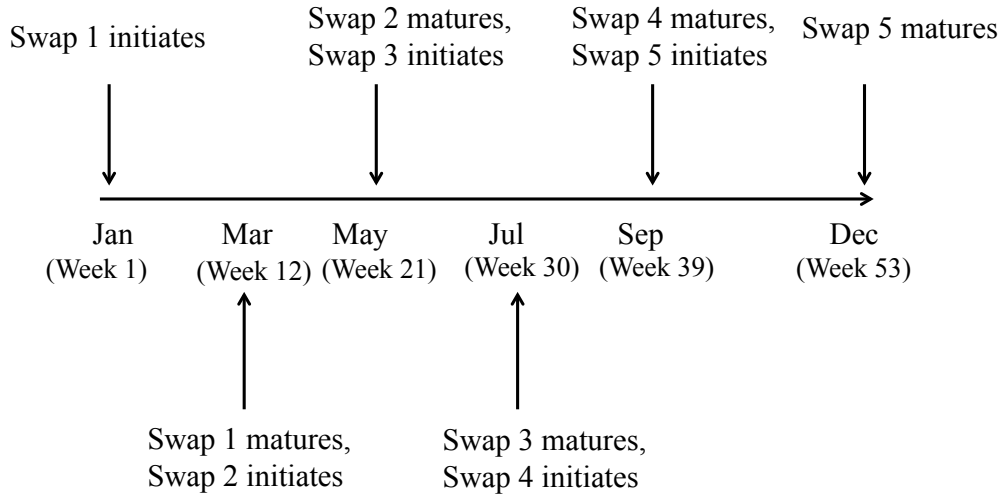


Figure 4.3: The sequence of the five swap contracts used in the model

contract, \overline{Ce}_q is priced by the following formula (Equation 4.16, [19]):

$$\sum_{t=T_1}^{T_N} \frac{\overline{Ce}_q}{(1+r_t)^t} = \sum_{t=T_1}^{T_N} \frac{Pe_t}{(1+r_t)^t} \quad (4.16)$$

where Pe_t is the time-varying ethanol spot price forecast at time t , r_t is the risk-free rate at time t , T_1 and T_N are the initial date and the maturity date of the swap contracts respectively. The fixed legs of the corn swap contract can be similarly priced.

4.3.4 A backtesting model to compare the realized profit and the negotiated profit

The backtesting model aims at implementing the strategy formulated in the optimization program with the real corn and ethanol spot price data. The resulting realized profit is then compared with the negotiated profit.

Therefore, the realized profit $\mathcal{P}\mathcal{r}$ is firstly calculated using Equation 4.17:

$$\begin{aligned} \mathcal{P}\mathcal{r} = & \sum_{q=1}^5 \overline{C}e_q H e_q + \sum_{t=1}^T \mathcal{P}e_t (prod_t - H e_q) - \sum_{q=1}^5 \overline{C}c_q H c_q \\ & - \sum_{t=1}^T \mathcal{P}c_t (f s_t - H c_q) - C f_2 \sum_{t=1}^T prod_t \end{aligned} \quad (4.17)$$

where $\mathcal{P}e_t$ and $\mathcal{P}c_t$ are the historical weekly spot price for corn and ethanol, Ce_q and Cc_q are the calculated fixed legs of the q -th ethanol/corn swap contracts, and He_q , $prod_t$, Hc_q , and fs_t are the optimal production and hedging variables obtained from the optimization program.

Similarly, the negotiated profit $\overline{P}r$ can be calculated using Equation 4.18:

$$\begin{aligned} \overline{P}c_{i,j} &= \frac{1}{T \cdot S} \sum_{i=1}^T \sum_{j=1}^S P c_{i,j} \\ \overline{P}e_{i,j} &= \frac{1}{T \cdot S} \sum_{i=1}^T \sum_{j=1}^S P e_{i,j} \\ \overline{P}r &= \sum_{t=1}^T \overline{P}e_{i,j} P cap - \sum_{t=1}^T \overline{P}c_{i,j} \frac{P cap}{C f_1} - C f_2 \sum_{t=1}^T P cap \end{aligned} \quad (4.18)$$

Since both the selling and purchasing prices are negotiated in advance, the producer's optimal strategy would be to produce at full capacity throughout the entire planning horizon. Therefore, the weekly facility production capacity, $Pcap$, is used and the corresponding supply of corn is calculated using the conversion

ratio Cf_1 . Finally, as the negotiated price information is generally proprietary, the spot price scenario mean, $\overline{P_{c_{i,j}}}$ and $\overline{P_{e_{i,j}}}$, are used as reasonable proxy.

Once the realized profit $\mathcal{P}\tau$ and the negotiated profit \overline{Pr} are obtained from Equation 4.17 and 4.18, the comparative advantage of the optimization model over the current practice can then be verified.

4.4 Results

In this section, the results related to the vector error correction model are discussed first. The second stage spot price processes are then represented with a sample of 1000 price trajectories from the VECM.

The stochastic program determines a portfolio of long-term strategies to maximize the total expected profit and has 108,180 variables and 108,170 constraints. For comparison purposes, the decisions and the profit distributions for both the risk neutral and risk averse case are first presented. As the operators are largely risk averse, the decisions for the risk averse case are then implemented to the target biorefinery with the real spot price datasets. Finally, the realized profit is compared with the negotiated profit. All the optimization models are solved with CPLEX 12.5.0.1.

4.4.1 Results for vector error correction model

All historical spot price data was obtained from [5]. The vector error correction model (VECM) assumes there exists cointegration between the two time series.

Therefore, it is important to first examine the validity of this assumption. The Engle-Granger Test tests the null hypothesis that there are no integrating relationships between the two series. Since a unique VECM is developed for each year from 2009 to 2015, the Engle-Granger Test is applied to each training series over these seven years. The test p value is shown in Table 4.2. All the p values are much smaller than 0.05, suggesting the null hypothesis can be rejected. Therefore, there is cointegration between the two series across the seven years.

Year	2009	2010	2011	2012	2013	2014	2015
p value	0.0345	0.0088	0.001	0.0275	0.0058	0.0031	0.0064

Table 4.2: p value for the Engle-Granger test from 2009 to 2015

Since, the parameters of VECM are estimated from the corresponding vector autoregressive model (VAR), a series of candidate VAR models ranging from order 1 to order 6 have been selected. Orders higher than 6 suffers from the potential of overfitting, thus are not considered. The order that has the lowest AIC value is chosen. Table 4.3 shows the order of the VECM.

Year	2009	2010	2011	2012	2013	2014	2015
model order	0	0	0	2	2	1	1

Table 4.3: Model order from 2009 to 2015

To visualize the parameters and validate the accuracy of the model forecast, the models with the end year 2009 and the end year 2015 are selected as demonstration. Table 4.4 illustrates the parameters and Figure 4.4 demonstrates the one year ahead forecast uncertainty range benchmarked on the real spot price.

The spot price forecast is obtained from averaging over one-year ahead Monte Carlo simulations. And the upper and lower uncertainty range are represented by the 95 and 5 percentile of the simulation. For almost all the weeks

End Year	C		B_1	
2009	-0.3089	0.0625	N.A.	
	-0.2166	-0.0632		
2015	-0.1206	0.0218	0.0867	0.0572
	-0.1150	-0.0040	0.0263	0.0597

Table 4.4: Model parameters of Year 2009 and Year 2015

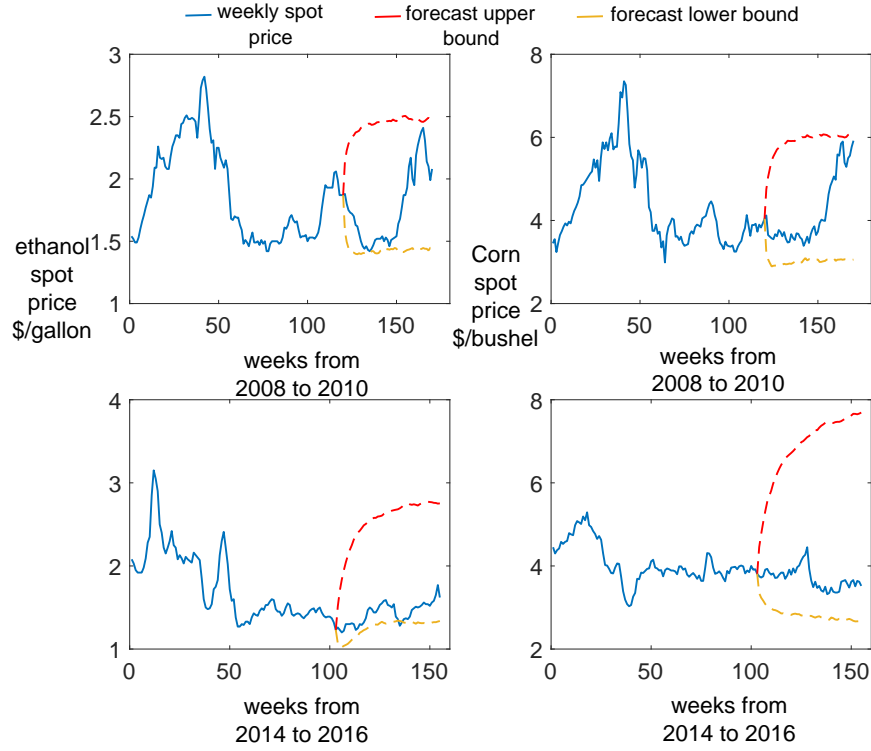


Figure 4.4: Monte Carlo forecast benchmarked on the real spot price, the forecast year is 2010 and 2016.

in 2010 and 2016, the real spot prices of both ethanol and corn falls within the uncertainty range.

In the following sections, the simulations are used as scenarios which are input to the optimization program.

4.4.2 Production schedule and hedging decisions for risk neutral and risk averse producer

In this section, the results of the stochastic optimization model are presented. The decisions for both the risk neutral and the risk averse operators are compared. Since the model is run for each year from 2010 to 2016 with the similar conclusion, the results for 2016 are presented here as a demonstration. For this purpose, the key parameter values for the case-study of 2016 are listed in Table 4.5.

The optimization model is solved using the price simulations and fixed legs determined in the previous sections. The risk neutral decisions are obtained by relaxing the risk management constraints (Equation 4.12-4.14), whereas the risk averse decisions are derived by adding the risk management constraints and setting K as 4.02×10^6 (Table 4.5). The decision variables in the first-stage are weekly corn supply, ethanol production and weekly hedging levels for each period. Figure 4.5 shows the profit distribution and the first-stage decisions for both the risk neutral and the risk averse producers. As the operator becomes risk averse, the ethanol production and corn supply is reduced. Specifically, the schedule to operate at full capacity is delayed to Week 6 instead of Week 5 for a risk averse producer. The other apparent difference lies in the hedging decisions. While the hedging level for a risk averse operator is always higher than that of a risk neutral operator, it is optimal for a risk averse operator to enter into full hedging after Week 13. In contrast, a risk neutral operator only chooses full hedging sporadically. Therefore, it can be concluded that the profit certainty for a biorefinery comes from two sources, first the decrease of the production level and second, the increase in using swap contracts.

Table 4.5: Case-Study Parameters for two-stage stochastic program

Parameter	Value
Scenario probability (π_j)	0.001 ¹
Conversion factor for corn swap (Q_c)	127 ton/share
Conversion factor for ethanol swap (Q_e)	125 ton/share
Production capacity ($Pcap$)	9.9 ton/hour
Coefficients for ethanol production level (Cf_1)	0.33
Operating cost coefficient (Cf_2)	0.5 \$/ton
1 st fixed leg of corn ($\overline{Cc_1}$)	4.36 \$/bushel
2 nd quarter fixed leg of corn ($\overline{Cc_2}$)	4.84 \$/bushel
3 rd quarter fixed leg of corn ($\overline{Cc_3}$)	5.06 \$/bushel
4 th quarter fixed leg of corn ($\overline{Cc_4}$)	5.16 \$/bushel
5 th quarter fixed leg of corn ($\overline{Cc_5}$)	5.23 \$/bushel
1 st fixed leg of ethanol ($\overline{Ce_1}$)	1.59 \$/gallon
2 nd quarter fixed leg of ethanol ($\overline{Ce_2}$)	1.90 \$/gallon
3 rd quarter fixed leg of ethanol ($\overline{Ce_3}$)	1.99 \$/gallon
4 th quarter fixed leg of ethanol ($\overline{Ce_4}$)	2.03 \$/gallon
5 th quarter fixed leg of ethanol ($\overline{Ce_5}$)	2.05 \$/gallon
User-defined risk preference level (K)	4.02×10^6 \$
Percentile of the profit distribution (α)	0.05

¹ Since every scenario is generated with equal weights, the probability for each scenario is $\frac{1}{N}$, where N is 1000 here.

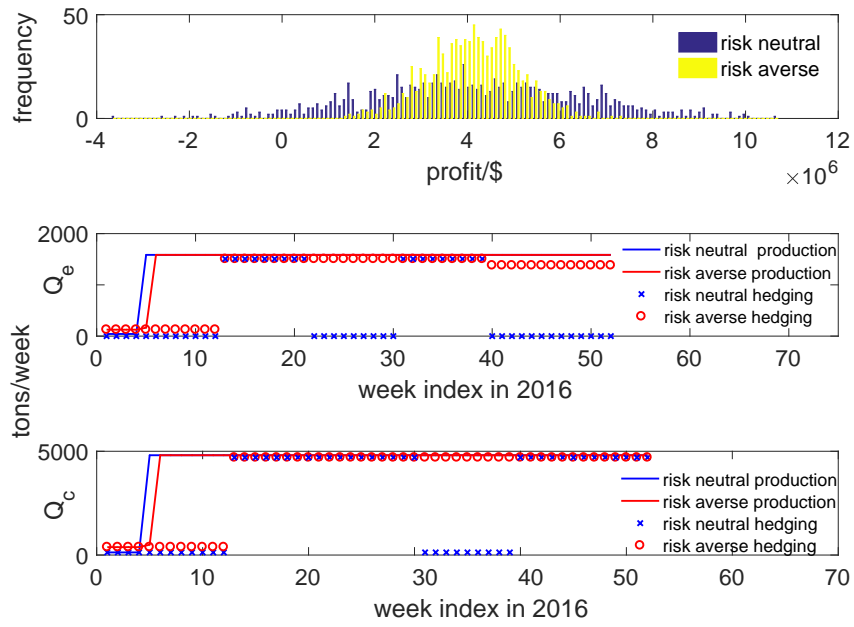


Figure 4.5: Profit distribution and operation strategies for risk neutral and risk averse operators, $Q_{c/e}$ represents the quantities of corn/ethanol per week

Example	$E[\text{profit}]/\text{million \$}$	normalized std
risk neutral	4.13	0.558
risk averse	4.12	0.234

Table 4.6: Expected profit and normalized standard deviation for risk neutral and risk averse operators

The differences in the operation decisions also lead to the variation in profit distributions. Specifically, the risk averse decisions, featured in less production and more hedging, result in higher profit certainty but lower expected profit level as shown in Table 4.6. This is also cross-validated by a more concentrated profit distribution shown in Figure 4.5. Hence, it is safe to conclude that the effective risk management can be achieved by using swap contracts and adjusting production levels. In the next section, a comparison of this approach to the current industry practice is delineated, and only the risk averse operator is considered due to the fact that the biorefinery operators in general are risk averse.

4.4.3 Backtesting results

In this section, the risk averse operation decisions obtained for each year from 2010 to 2016 are implemented in the modeled plant with the real spot price data. The realized profit is calculated and subsequently compared with the negotiated profit. The top plot in Figure 4.6 presents the profit comparisons of hedging with swap contract (realized profit) and using current practice (fixed rate). The realized profit obtained from implementing the optimal operation decisions is higher than that of adopting current practice across all the years. The reason for the profit improvement is shown in the middle and bottom plot of Figure 4.6. To fully explain the profit improvement, “margin” is defined first in Equation 4.19, which is the price difference between the ethanol produced from one ton

of corn.

$$\text{margin} = P_e \times Cf_1 - P_c \quad (4.19)$$

In the years when the margins are relatively high, for example 2010, 2011, and 2014, the optimal decisions allow part of the product sold on the spot market or sold by a series of swap contracts rather than solely on a long-term fixed rate price. The potential decision flexibility gives rise to the additional profit. On the contrary, during the years when the margin is low (2012, 2013 and 2016), the optimal decisions determine the production only on favorable weeks. Furthermore, full hedging is entered over most of the weeks to provide another layer of profit protection. To conclude, with the optimization model, risk averse producers are better informed of the correct production timing and level rather than blindly producing at full capacity regardless of the market conditions. Additionally, the use of swap contract protects the operators from directly facing the price fluctuations in the spot market.

It is also worth noting that since the biorefinery operators generally prefer simple and feasible operation decisions, the production and hedging strategies formulated in the optimization model turn out to satisfy their preference. With the help of the optimization model, the operator would be able to schedule the demand for corn and production of ethanol in the beginning of the planning horizon, and then enter into full hedging with swap contracts on both supply and demand side.

Finally, as the fixed rate price of the current practice is approximated via using one-year ahead forecast, it is necessary to implement a sensitivity analysis

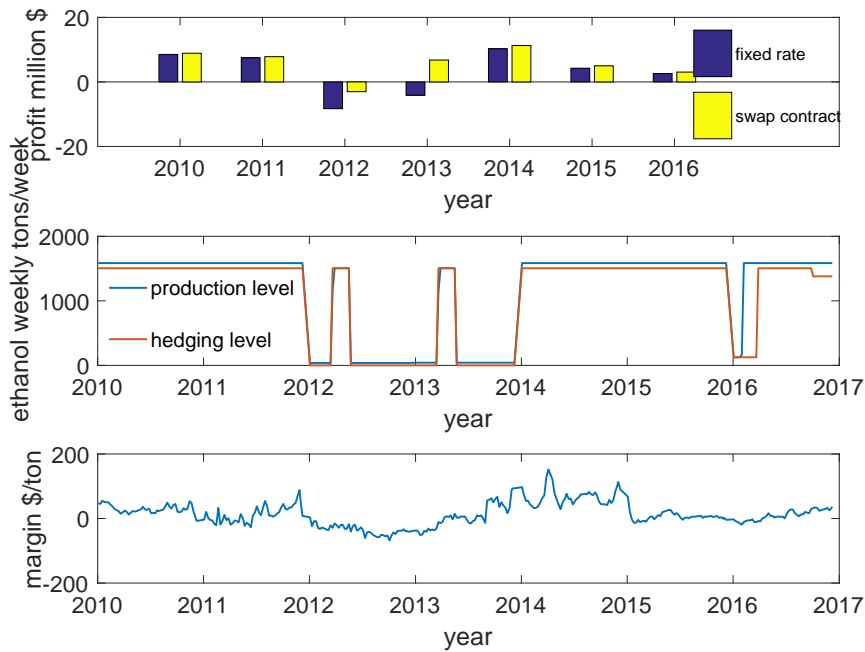


Figure 4.6: Top figure: profit comparison, middle figure: production and product hedging decisions for risk averse operator, bottom figure: profit margin

with respect to these fixed rate prices. For both the corn and ethanol fixed rate prices from 2010 to 2016, the prices are raised above 5% and below 5%, which is the typical annual volatility of commodity prices. And the profit difference is defined as the difference between the realized profit and the negotiated profit.

It can be observed from Figure 4.7 that while the negotiated profit is slightly higher than the realized profit if the ethanol/corn fixed rate is raised/decreased by 5% in the high margin years, the negotiated profit is still much less than the realized profit in the low margin years. Undoubtedly, the negotiated profit is always a lot less than the realized profit if the ethanol/corn fixed rate is dropped/increased by 5%. Although it is hardly possible to find a set of oper-

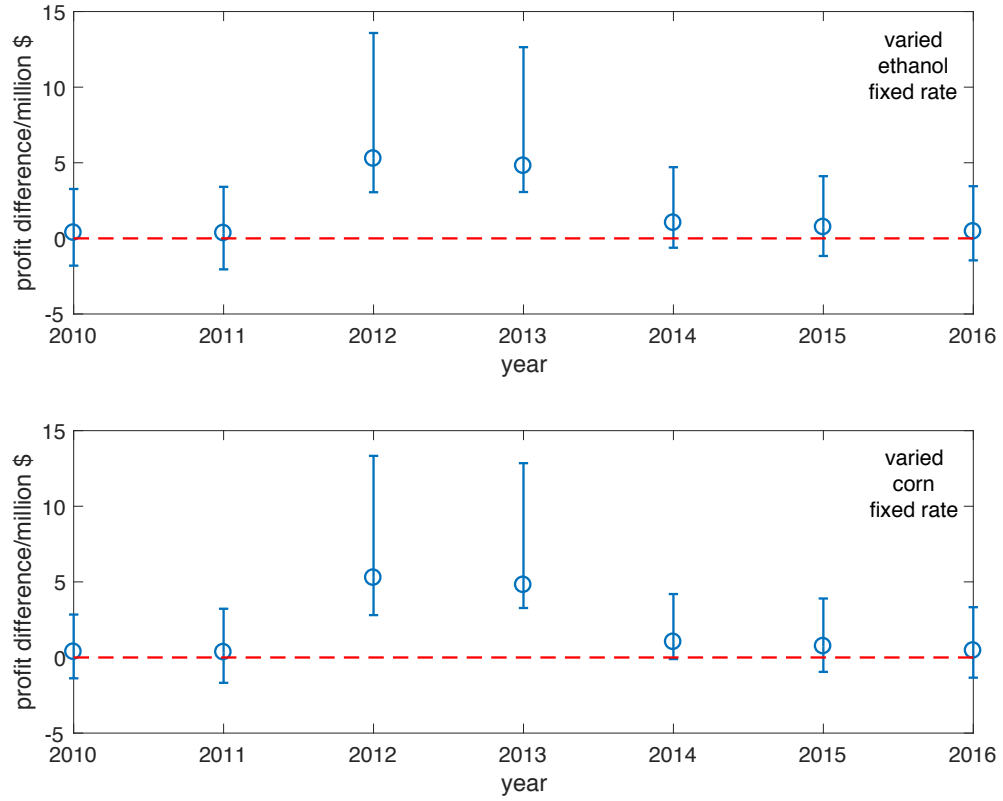


Figure 4.7: Impact of changing the fixed rate prices on the profit difference, where the profit difference is defined as realized profit, \mathcal{P}_t , less the negotiated profit, \overline{P}_r

ation decisions that perform consistently better within a wide sensitivity range and under all the market conditions, the operation decisions that constantly protect the operators from adverse market conditions within a wide sensitivity range would still be preferable for risk averse operators.

4.5 Conclusion

This study has presented a framework to determine the optimal corn supply, ethanol production, and hedging decisions for a corn biorefinery. A two-stage

stochastic program has been formulated in light of the decision sequence, while the underlying correlated spot prices are characterized by a vector error correction model. The optimal operation decisions for both risk neutral and risk averse operators are compared first. And it has been demonstrated that with the increase of risk aversion level, the operator chooses to decrease the ethanol production level and increase the use of both corn and ethanol swap contracts. In this way, a more concentrated profit distribution is obtained although lower expected profit is achieved.

Given the biorefinery operators are generally risk averse, the decisions for the risk averse operators are back tested in the backtesting model with real spot price data from 2010 to 2016. The realized profit is compared with the negotiated profit acquired from the current industry practice, that is, negotiating long-term fixed rate prices for both corn and ethanol. The comparison shows the superiority of the realized profit throughout the entire testing horizon. And it is further illustrated that this improvement is due to the decision flexibility and informed control of production timing and level.

Finally, a sensitivity analysis regarding to the negotiated fixed rate prices has been implemented. The result shows the operation decisions derived from the optimization framework are better suited for the risk averse operators due to their ability to protect the operators within a wide sensitivity range in low margin years.

CHAPTER 5

CONCLUSION

Three projects are presented in this work, each of which considers different optimal production and hedging strategies to maximize the process profit of a biorefinery, under three different situations or configurations. The first study presents a two-phase stochastic programming model to determine the short-term production schedule and forward hedging portfolio for a biochemical lignocellulosic biorefinery. The carbon tax constraints are considered to meet the increasing stringent environmental regulations. In the second study, the model framework resolves to find the long-term production and hedging strategy for the same biochemical lignocellulosic biorefinery. The model framework includes a two-factor time series model and a two-stage stochastic programming model. The time series model takes into account the long-term dynamics of ethanol spot prices, whereas the optimization model determines the weekly production level and quarterly swap contract hedging level. Furthermore, the relationship between production, spot price, carbon tax, and storage capacity has been fully explored. Sensitivity analysis of spot price dynamics and storage capacity are also investigated. In the third study, a similar framework is developed to determine the long-term production and hedging strategy for a first generation corn biorefinery. Different from the second generation lignocellulosic biorefinery, the price uncertainty of a first generation biorefinery comes from both the feedstock and the product. Therefore, the model consists of a vector time series model and a two-stage stochastic programming model. While the time series model characterizes the long term dynamics for both the corn and ethanol spot prices, the two-stage stochastic programming model generates the optimal weekly production level and swap contracts portfolios for both

corn and ethanol. More importantly, the optimal decisions are backtested using the historical spot price from 2010 to 2016. The calculated realized profit is subsequently compared with the negotiated profit to demonstrate the advantage of the model framework.

The key findings from these studies are:

1. The tradeoff between the price certainty and expected profit level has been observed unanimously throughout the three studies. Since the biorefinery operators are generally risk averse, the optimal strategy is to enter into forward/swap contracts to lock in the purchasing/selling prices and produce less during the periods with low ethanol spot prices.
2. In short-term decision making, the use of forward contract becomes a dominant factor to determine the production patterns. It is optimal to produce more whenever the forward contract price is high. However, long-term production pattern is influenced by several different factors, namely, ethanol expected spot price, carbon tax, and storage capacity. Specifically, a low expected ethanol spot price and carbon tax rate, as well as the ability to store increase the production level.
3. The model framework developed for long-term risk management is able to generate customized production and hedging strategies for operators of different risk preferences. The most risk averse producers would fully hedge their feedstock/product and produce at “safe” periods when the expected ethanol spot prices are high.
4. The storage capability serves as a buffer to the process. A higher storage capacity reduces the operators’ reliance on financial derivatives, and increases the process profit. This represents a tradeoff between “hedge for

now” and “store for later sale”.

5. There exists a threshold price for the expected ethanol spot price such that whenever the price drops below the threshold price, the production level decreases.
6. The optimization model framework is shown to outperform the current industry practice in terms of realized profit in each year from 2010 to 2016. This improvement is due to a combination of using financial derivatives, correct production timing, and optimal production level.

Overall, this thesis presents a systematic methodology to assist the biorefinery operators to maximize the process profit and manage the price risk both in the short-term and long-term. Feasible and customized production and hedging decisions can be obtained by using the model framework developed in this thesis. To take the further environmental regulation into account, carbon tax constraints are formulated into the model. It is the author’s hope that the results obtained from this thesis can first alert the industry practitioners that flexible production schedule and use of financial derivatives, albeit bringing a small degree of uncertainty, increase the possibility of gaining extra profit. Second, it is promising for the industry practitioners to achieve higher financial sustainability by adopting the decisions determined from the model.

BIBLIOGRAPHY

- [1] Agricultural Marketing and Resource Center. Midwest ethanol cash prices, basis data, and charts for selected states, February 2014.
- [2] Richard C Baliban, Josephine A Elia, Christodoulos A Floudas, Barri Guirau, Michael B Weingarten, and Stephen D Klotz. Hardwood biomass to gasoline, diesel, and jet fuel: 1. process synthesis and global optimization of a thermochemical refinery. *Energy & Fuels*, 27(8):4302–4324, 2013.
- [3] Andres Barbaro and Miguel J Bagajewicz. Managing financial risk in planning under uncertainty. *AIChE Journal*, 50(5):963–989, 2004.
- [4] Saif Benjaafar, Yanzhi Li, and Mark Daskin. Carbon footprint and the management of supply chains: Insights from simple models. *IEEE transactions on automation science and engineering*, 10(1):99–116, 2012.
- [5] Bloomberg L.P. Weekly new york ethanol (platts) futures and spot price from november 2006 to september 2014, 2014.
- [6] Alessio Boldrin and Thomas Astrup. Ghg sustainability compliance of rapeseed-based biofuels produced in a danish multi-output biorefinery system. *Biomass and Bioenergy*, 75:83–93, 2015.
- [7] Bruno A Calfa and Ignacio E Grossmann. Optimal procurement contract selection with price optimization under uncertainty for process networks. *Computers & Chemical Engineering*, 82:330–343, 2015.
- [8] ALARS Carvalho. Calibration of the schwartz-smith model for commodity prices. *Instituto de Matemática Pura e Aplicada (Brasil)*, 2010.
- [9] Peam Cheali, Alberto Quaglia, Krist V Gernaey, and Gurkan Sin. Effect of market price uncertainties on the design of optimal biorefinery systems-a systematic approach. *Industrial & Engineering Chemistry Research*, 53(14):6021–6032, 2014.
- [10] Yang Chen. *Optimal design and operation of energy polygeneration systems*. PhD thesis, Massachusetts Institute of Technology, 2012.
- [11] Lingfeng Cheng and C Lindsay Anderson. Financial sustainability for a lignocellulosic biorefinery under carbon constraints and price downside risk. *Applied Energy*, 177:98–107, 2016.

- [12] Lingfeng Cheng, MG Martínez, and CL Anderson. Long term planning and hedging for a lignocellulosic biorefinery in a carbon constrained world. *Energy Conversion and Management*, 126:463–472, 2016.
- [13] US DoE. Buildings energy databook. *Energy Efficiency & Renewable Energy Department*, 2011.
- [14] Michael Duffy. Estimated costs for production, storage, and transportation of switchgrass. Technical report, Iowa State University, Department of Economics, 2007.
- [15] Robert F Engle and Clive WJ Granger. Co-integration and error correction: representation, estimation, and testing. *Econometrica: journal of the Econometric Society*, pages 251–276, 1987.
- [16] EPA. Renewable fuel standard program, July 2016.
- [17] Katie Fehrenbacher. As kior crashes, it’s another cautionary tale for energy innovation, May 2014.
- [18] Salahedden Moftah Gadmor. *Hedging with derivatives in the oil industry*. PhD thesis, Simon Fraser University, 2006.
- [19] Gerald Gay, Anand Venkateswaran, Robert W Kolb, and James A Overdahl. The pricing and valuation of swaps. *Financial Derivatives: Pricing and Risk Management*, pages 405–422, 2008.
- [20] A Geraili, P Sharma, and JA Romagnoli. Technology analysis of integrated biorefineries through process simulation and hybrid optimization. *Energy*, 73:145–159, 2014.
- [21] Aryan Geraili and Jose A Romagnoli. A multiobjective optimization framework for design of integrated biorefineries under uncertainty. *AIChE Journal*, 61(10):3208–3222, 2015.
- [22] Dominice Goodwin. Schwartz-smith two-factor model in the copper market: before and after the new market dynamics. 2013.
- [23] D Gregg and JN Saddler. Bioconversion of lignocellulosic residue to ethanol: process flowsheet development. *Biomass and Bioenergy*, 9(1-5):287–302, 1995.

- [24] Warren J Hahn, James A DiLellio, and James S Dyer. What do market-calibrated stochastic processes indicate about the long-term price of crude oil? *Energy Economics*, 44:212–221, 2014.
- [25] Carlo N Hamelinck, Geertje Van Hooijdonk, and Andre PC Faaij. Ethanol from lignocellulosic biomass: techno-economic performance in short-, middle-and long-term. *Biomass and bioenergy*, 28(4):384–410, 2005.
- [26] Andrew C Harvey. *Forecasting, structural time series models and the Kalman filter*. Cambridge university press, 1990.
- [27] C John Hull. *Options futures & other derivatives*. 2008.
- [28] D. Humbird, R. Davis, L. Tao, C. Kinchin, D. Hsu, A. Aden, P. Schoen, J. Lukas, B. Olthof, M. Worley, D. Sexton, and D. Dudgeon. Process design and economics for biochemical conversion of lignocellulosic biomass to ethanol: Dilute-Acid Pretreatment and Enzymatic Hydrolysis of Corn Stover. *Contract*, 303:275–3000, 2011.
- [29] Xiaocong Ji, Simin Huang, and Ignacio E Grossmann. Integrated operational and financial hedging for risk management in crude oil procurement. *Industrial & Engineering Chemistry Research*, 54(37):9191–9201, 2015.
- [30] Natasha Kirby and Matt Davison. Using a spark-spread valuation to investigate the impact of corn-gasoline correlation on ethanol plant valuation. *Energy Economics*, 32(6):1221–1227, 2010.
- [31] Pavlo Krokmal, Jonas Palmquist, and Stanislav Uryasev. Portfolio optimization with conditional value-at-risk objective and constraints. *Journal of risk*, 4:43–68, 2002.
- [32] Jan Larsen, Mai Østergaard Haven, and Laila Thirup. Inbicon makes lignocellulosic ethanol a commercial reality. *Biomass and Bioenergy*, 46:36–45, 2012.
- [33] James A Larson, Burton C English, Lixia He, et al. Risk and return for bioenergy crops under alternative contracting arrangements. In *Southern Agricultural Economics Association Annual Meeting, Dallas, Texas, February*, pages 2–6, 2008.
- [34] Yihua Li, Chung-Li Tseng, and Guiping Hu. Is now a good time for iowa to invest in cellulosic biofuels? a real options approach considering construc-

tion lead times. *International Journal of Production Economics*, 167:97–107, 2015.

- [35] Mariano Martín and Ignacio E Grossmann. Energy optimization of bioethanol production via gasification of switchgrass. *AIChE Journal*, 57(12):3408–3428, 2011.
- [36] Mariano Martín and Ignacio E Grossmann. Energy optimization of bioethanol production via hydrolysis of switchgrass. *AIChE Journal*, 58(5):1538–1549, 2012.
- [37] Mariano Martín and Ignacio E Grossmann. On the systematic synthesis of sustainable biorefineries. *Industrial & Engineering Chemistry Research*, 52(9):3044–3064, 2012.
- [38] Christian Maxwell and Matt Davison. Using real option analysis to quantify ethanol policy impact on the firm’s entry into and optimal operation of corn ethanol facilities. *Energy Economics*, 42:140–151, 2014.
- [39] Christian Maxwell and Matt Davison. Real options with regulatory policy uncertainty. In *Commodities, Energy and Environmental Finance*, pages 239–273. Springer, 2015.
- [40] Andrew McAloon, Frank Taylor, Winnie Yee, Kelly Ibsen, and Robert Wooley. Determining the cost of producing ethanol from corn starch and lignocellulosic feedstocks. *National Renewable Energy Laboratory Report*, 2000.
- [41] Mat McDermott. World’s largest ethanol producer, verasun energy corp, files for bankruptcy, November 2008.
- [42] Marcelo Moreira, Angelo C Gurgel, and Joaquim EA Seabra. Life cycle greenhouse gas emissions of sugar cane renewable jet fuel. *Environmental science & technology*, 48(24):14756–14763, 2014.
- [43] Kimberley A Mullins, W Michael Griffin, and H Scott Matthews. Policy implications of uncertainty in modeled life-cycle greenhouse gas emissions of biofuels. *Environmental science & technology*, 45(1):132–138, 2011.
- [44] Jeongho Park, Sunwon Park, Choamun Yun, and Young Kim. Integrated model for financial risk management in refinery planning. *Industrial & Engineering Chemistry Research*, 49(1):374–380, 2009.

- [45] LG Pereira, MOS Dias, AP Mariano, R Maciel Filho, and AMFLJ Bonomi. Economic and environmental assessment of n-butanol production in an integrated first and second generation sugarcane biorefinery: Fermentative versus catalytic routes. *Applied Energy*, 160:120–131, 2015.
- [46] Lucas G Pereira, Marina OS Dias, Heather L MacLean, and Antonio Bonomi. Investigation of uncertainties associated with the production of n-butanol through ethanol catalysis in sugarcane biorefineries. *Bioresource technology*, 190:242–250, 2015.
- [47] Steven Phillips, Andy Aden, J Jechura, D Dayton, and T Eggeman. Thermochemical ethanol via indirect gasification and mixed alcohol synthesis of lignocellulosic biomass. *National Renewable Energy Laboratory, Golden, CO, NREL Technical Report No. TP-510-41168*, <http://www.nrel.gov/docs/fy07osti/41168.pdf>, 2007.
- [48] Chiara Piccolo and Fabrizio Bezzo. A techno-economic comparison between two technologies for bioethanol production from lignocellulose. *Biomass and bioenergy*, 33(3):478–491, 2009.
- [49] José María Ponce-Ortega, Viet Pham, Mahmoud M El-Halwagi, and Amro A El-Baz. A disjunctive programming formulation for the optimal design of biorefinery configurations. *Industrial & Engineering Chemistry Research*, 51(8):3381–3400, 2012.
- [50] Arkadej Pongsakdi, Pramoch Rangsunvigit, Kitipat Siemanond, and Miguel J Bagajewicz. Financial risk management in the planning of refinery operations. *International Journal of Production Economics*, 103(1):64–86, 2006.
- [51] R Tyrrell Rockafellar and Stanislav Uryasev. Conditional value-at-risk for general loss distributions. *Journal of Banking & Finance*, 26(7):1443–1471, 2002.
- [52] Sergey Sarykalin, Gaia Serraino, and Stan Uryasev. Value-at-risk vs. conditional value-at-risk in risk management and optimization. *Tutorials in Operations Research. INFORMS, Hanover, MD*, 2008.
- [53] Todd M Schmit, Jianchuan Luo, and Jon M Conrad. Estimating the influence of us ethanol policy on plant investment decisions: A real options analysis with two stochastic variables. *Energy Economics*, 33(6):1194–1205, 2011.

- [54] Todd M Schmit, Jianchuan Luo, and Loren W Tauer. Ethanol plant investment using net present value and real options analyses. *biomass and bioenergy*, 33(10):1442–1451, 2009.
- [55] Eduardo Schwartz and James E Smith. Short-term variations and long-term dynamics in commodity prices. *Management Science*, 46(7):893–911, 2000.
- [56] Teresa Serra and David Zilberman. Biofuel-related price transmission literature: A review. *Energy Economics*, 37:141–151, 2013.
- [57] Alexander Shapiro, Darinka Dentcheva, et al. *Lectures on stochastic programming: modeling and theory*, volume 16. SIAM, 2014.
- [58] Douglas HS Tay, Denny KS Ng, Norman E Sammons Jr, and Mario R Eden. Fuzzy optimization approach for the synthesis of a sustainable integrated biorefinery. *Industrial & Engineering Chemistry Research*, 50(3):1652–1665, 2011.
- [59] Richard SJ Tol. The social cost of carbon: trends, outliers and catastrophes. *Economics: The Open-Access, Open-Assessment E-Journal*, 2, 2008.
- [60] Janske van Eijck, Bothwell Batidzirai, and André Faaij. Current and future economic performance of first and second generation biofuels in developing countries. *Applied Energy*, 135:115–141, 2014.
- [61] Robert Wooley, Mark Ruth, John Sheehan, Kelly Ibsen, Henry Majdeski, and Adrian Galvez. Lignocellulosic biomass to ethanol process design and economics utilizing co-current dilute acid prehydrolysis and enzymatic hydrolysis current and futuristic scenarios. Technical report, DTIC Document, 1999.
- [62] Fengqi You, Ling Tao, Diane J Graziano, and Seth W Snyder. Optimal design of sustainable cellulosic biofuel supply chains: multiobjective optimization coupled with life cycle assessment and input–output analysis. *AIChE Journal*, 58(4):1157–1180, 2012.
- [63] Choamun Yun, Young Kim, Jeongho Park, and Sunwon Park. Optimal procurement and operational planning for risk management of an integrated biorefinery process. *Chemical Engineering Research and Design*, 87(9):1184–1190, 2009.

- [64] Qiao Zhang, Jian Gong, Matthew Skwarczek, Dajun Yue, and Fengqi You. Sustainable process design and synthesis of hydrocarbon biorefinery through fast pyrolysis and hydroprocessing. *AIChE Journal*, 60(3):980–994, 2014.
- [65] Suping Zhang, François Maréchal, Martin Gassner, Zoé Périn-Levasseur, Wei Qi, Zhengwei Ren, Yongjie Yan, and Daniel Favrat. Process modeling and integration of fuel ethanol production from lignocellulosic biomass based on double acid hydrolysis. *Energy & fuels*, 23(3):1759–1765, 2009.
- [66] Edwin Zondervan, Mehboob Nawaz, André B de Haan, John M Woodley, and Rafiqul Gani. Optimal design of a multi-product biorefinery system. *Computers & Chemical Engineering*, 35(9):1752–1766, 2011.